Response to Review comments 1 – Pablo Rodriguez-Salgado

We thank the reviewer for their overall positive comment on the manuscript

"I consider that this manuscript contributes to improve the general understanding of the mechanisms and styles of basin inversion. More specifically, this manuscript contributes with new data and observations to the knowledge of the Late Cretaceous – Cenozoic basin inversion and exhumation episodes in the Norwegian-Danish continental shelf. For that reason, I recommend publication of the manuscript after addressing few minor revisions."

We have responded to the individual comments and points raised by the reviewer below and included the changes in the revised manuscript, as shown in the attached track changes document. Our responses are shown in italics with line numbers corresponding to changes in the track changes document with full markup shown.

Reviewer comments and *responses:*

1) Is the formation pressure of lower Cretaceous interval is hydrostatic in the 7 wells selected for this study? Have the authors performed any pre-conditioning of the sonic log curve (e.g. removal of anomalous DT readings)?

Response

- *No overpressure was recorded within the Lower Cretaceous interval across the wells used in this study, hence we assumed that the Lower Cretaceous interval formation pressure was hydrostatic. This is consistent with regional studies which also show no signs of overpressure in this interval (e.g. Japsen et al., 1998). Additional text, explaining the hydrostatic nature of the wells has been added to the revised manuscript (Line 245-249)*
- *The sonic log curve was pre-conditioned prior to being incorporated into our analyses (Line 268-269) in order to remove any anomalous values. We have now clarified the text on lines 255-258 to better illustrate the pre-conditioning of the log prior to analysis.*

2) Can the authors provide further details about the geometry and orientation of the strike-slip fault zone along the Farsund North Fault? Although some details are given in the line 257 "The proposed strike-slip fault continues towards Domain A to the west, and continues to the southeast, south of Domain C, to the east." I think the manuscript could be improved by indicating the location of the strike-slip faults in the Figure 5a.

- *Due to erosion at the base Jurassic unconformity, which removes related growth strata, the presence of the strike slip faults can only be determined by the offsets between older (i.e. Permo-Triassic), N-S- striking faults. We have revised manuscript to make this clearer (Line 128-130).*
- *We can confirm the location of an older (i.e. pre-Cretaceous) strike-slip fault between offset N-S-striking faults, i.e. the fault partitioning the Farsund Basin and the fault along the western margin of the Varnes Graben. However, we can also show that no pre-cursor (i.e. Early-Middle Jurassic), strike-slip faulting occurred along the eastern segment of the Farsund North Fault, which initiated during the Early Cretaceous; we therefore suggest that the strike-slip system continued eastwards with a NW trend. A similar relationship occurs along the southern margin of the Farsund Basin, with the strike-slip system, the position and offset of which is constrained by the offset N-S-striking faults, interpreted to continue north of an*

Early Cretaceous segment of the Fjerritslev South Fault with a NW-SE strike (Phillips et al., 2018). Additional information has been included in the manuscript (Lines 298-313, 320-330) to better illustrate our constraints on the overall geometry of the strike-slip fault system. We also link our observations made here from the northern basin margin to complementary observations from the southern basin margin (see Phillips et al., 2018).

- *We have added a proposed continuation of the strike-slip system to Figure 5a to make the relationship between it and the eastern segment of the Farsund North Fault (Domain C) clearer.*

3) Line 270 – "We suggest that Domain C represents an Early Cretaceous segment of the Farsund North Fault, which propagated away from a pre-existing segment (Domain A) during the Early Cretaceous, with Domain B situated between the two segments." I completely agree. However, I think that segmentation along the Farsund North Fault is an important point and it could be further developed in the text. Is there any evidence of fault segmentation in the throw-distance profile shown in the Fig. 5b? For example, displacement patterns in this figure show throw maxima in the central part of the domains A and C decreasing towards the domain B. Also, a similar throw pattern is observed between the domains C and D. Could these patterns reflect different kinematically linked segments? Is there any relay ramp observed between the domains A and C and the domains C and D? In the TWT structure map (Fig 5a) the authors show the Farsund North Fault as a continuous structure. Can the authors show the fault segments mentioned in the text (e.g. lines 270 and 349)? Also, can these segments be shown in the interpreted seismic sections (Figs 5a and 8a)?

- *We agree that segmentation along the Farsund North Fault, as represented by the present distribution of throw, is an important point that was underexplored in the initial manuscript. In the revised manuscript we discuss in greater detail the geometry and distribution of throw along this fault 1 (Lines 299-301; 344-348).*
- *We note throw maxima in the centre of domains A and C, and suggest that these likely reflect segmentation of the initial fault, particularly as the eastern fault segment did not reactivate a pre-existing strike slip fault (see response to point 2).*
- *Relay ramp segmentation is likely present between Domain B and Domain C. We suggest that the segment in Domain C propagated away from Domain B (where we know a strike-slip precursor fault was present, see point 2) during the Early Cretaceous, rather than representing a segment that subsequently linked with the one in Domain B.*
- *Domain D largely covers the Agder slope, east of the Farsund North Fault, although the eastern termination of the eastern fault segment (i.e. the segment that characterises Domain C) extends into the western end of Domain D (Line 351).*

4) I understand that whereas both (fault) segments were active at least since Early Cretaceous times, there is no evidence that the Farsund North Fault was active during Carboniferous-Permian times. Is there any other evidence of Carboniferous-Permian activity (i.e. growth of the sequences) recorded by any other E-W-striking faults in the area? I think this could be an important point to be added to the conclusions.

Response

- *Extensional faults defining the Farsund Basin are largely not present during pre-Zechstein extension (See Figure 3), in contrast to elsewhere along the Sorgenfrei-Tornquist Zone, where faults were active during Carboniferous-Permian extension. We can also confirm that the eastern segment of the Farsund North Fault was Early Cretaceous or younger in age.*
- *We note that the western segment of the Farsund North Fault was likely active during Early-Middle Jurassic strike-slip activity, with the Farsund North Fault showing a similar geometric*

and kinematic relationship to that of the Fjerritslev Fault System along the southern basin margin and propagating away from the strike-slip structure (see response to point 2). However, due to erosion at the BJU across the Upper Terrace of the Farsund Basin, we are unable to determine whether this area and associated faults experienced earlier, Carboniferous-Permian activity. We note that Carboniferous-Permian extension has been documented elsewhere along the Tornquist Zone (e.g. Erlstrom et al., 1997), and is also documented to the west in the Egersund Basin (Jackson and Lewis, 2013) (Line 117).

- *We have revised the manuscript to better outline the evolutionary histories of the various fault segments and to also better convey the uncertainty regarding Carboniferous-Permian activity along the Farsund North Fault, particularly along the western segment (Line 322-325, 442-445).*

5) Is there a null-point observed in any of the Lower Cretaceous or older horizons along the Farsund North Fault? I think it is worth mentioning in the manuscript whether this observation is made or not.

Response

- *We do not identify a null point at any point along the Farsund North Fault as the magnitude of the initial extensional offset along the fault was much greater than the subsequent reverse offset. Therefore, the fault displays net-extensional offset at all depths. We have included this important point in the revised manuscript (Line 417-419)*

6) Whereas the authors interpret a Late Cretaceous age for the inversion and exhumation in the Farsund Basin (Line 419) I understand that magmatic underplating is the main uplift mechanism behind the Neogene exhumation episode (e.g. paragraph starting in Line 425). However, in some parts of the manuscript the authors include both the Late Cretaceous and Neogene episodes within the term basin inversion.
As the term basin inversion implies that uplift is controlled by reverse reactivation of a pre-existing fault system (Cooper et al., 1989). This excludes any other source of uplift not caused by compressional reactivation of pre-existing faults (Chadwick et al., 1993) I think therefore that the use of the term basin inversion in some parts of the manuscript should be revised.

Response

- *We agree with the points raised by the reviewer here that the term "basin inversion" should not be used to describe the Neogene uplift event, and that this event should be clearly distinguished from the earlier, Cretaceous event. Furthermore, as we are unable to distinguish between individual uplift pulses, including those that may have occurred earlier in the Paleogene, we now refer to 'Paleogene-Neogene uplift' rather than 'Neogene inversion' to encompass all post Cretaceous uplift (e.g. lines 102, 138, 495). We also agree with the reviewer regarding our mode general use of the term "basin inversion". Following additional comments from reviewer 2, we have modified our usage of this term. We now refer to Late Cretaceous "compression" or "shortening", which we argue were expressed via a number of different mechanisms across the Farsund Basin, including basin inversion (which was explicitly associated reverse reactivation of basin-bounding normal faults). This has been modified in the revised manuscript (e.g. Lines 30-42).*

Additional minor and textual changes have been completed throughout the manuscript.

Review 2 – Fabian Jahne-Klingberg

We thank the reviewer for their detailed and thorough review of the manuscript and their positive comments:

"The subject matter is well presented in the manuscript. Most illustrations contribute to understanding of the manuscript in their current form. The manuscript provides important new insights into the structural development along the STZ. For this reason I recommend publishing the manuscript after moderate revisions have been made."

We have responded to the individual comments made by the reviewer below and have made changes accordingly in the track changes document. Our responses are shown in italics with line number corresponding to the full markup document. Revised figures are also attached to this document. We believe that these comments and our associated changes have greatly improved the manuscript.

Many thanks,
Thomas Phillips

Reviewer comments and *responses:*

1. The authors should explain more clearly their definition of "inversion" and "reactivation". Are all the interpreted parts of the structure which show uplift/erosion are inverted? Or is inversion one structural style of shortening along the whole structure?
Is inversion the effect of shortening or as well of other processes? Is the term "inversion" used as umbrella for structural inversion as well for basin inversion? Compressional/transpressional reactivation/shortening is perhaps the better umbrella term.

Response -
See also response to point 6 of reviewer 1.
We have amended the terms that we use throughout the manuscript. We agree that 'inversion' represents just one mechanism that accommodates shortening along the northern basin margin. We have followed the definition from Williams and Turner (1989) with regards to inversion being the process by which previously extensional structures experience uplift and compression (Line 30-32). We have modified the manuscript, particularly in the introduction to state the different mechanisms by which compression and shortening can be accommodated, including the reverse reactivation of faults, and the inversion of previously extensional basins (Line 32-34). Specific changes can be found in response to the comments from the annotated pdf.

2. Can the uplift, especially the Neogene, be explained by other processes as shortening (e.g. dynamic topography)? And can the Neogene Uplift which is not clearly related to structures or basins really be called inversion?

Response -
We agree that the Paleogene-Neogene uplift is not necessarily related to inversion and shortening, and have since modified this in the revised manuscript in response to other

comments (i.e. points 1, 4). As we are unable to distinguish between individual uplift events throughout the Cenozoic we now refer to these uplift phases collectively as Paleogene-Neogene uplift.
We outline some proposed causes of the Paleogene and Neogene uplift events, including upper mantle motions and dynamic topography (Line 150) and also plate tectonic forces associated with the opening of the North Atlantic (Line 150-151). We note that whilst Late Cretaceous compression is amplified along the STZ, the STZ represents a relative hingeline during Paleogene-Neogene uplift, separating areas of relatively high and low uplift.

3. Not the Alpine-Carpathian orogeny is the reason for Late Cretaceous shortening of structures in the CEBS, but it's the result from Africa-Iberia-Europe convergence. Greater parts of the alps show an extensional setting during the Cretaceous. But the Pyrenees were active during this time.

Response -
We thank the reviewer for raising this point that it is not the Alpine-Carpathian orogeny that is responsible for the Late Cretaceous compression, rather the convergence of Africa, Iberia and Europe, as outlined by Kley and Voigt (2008). As such, we now relate Late Cretaceous compression to Africa-Iberia-Europe convergence rather than the Alpine Orogeny throughout the manuscript (e.g. Line 83-84, 140, 502, 545).

4. Please avoid "unclear relations", generalisations like: - Late Cretaceous inversion (Late Cretaceous shortening has not only produced inversion structures.) – Neogene shortening (the mechanism behind Neogene uplift is still under discussion) – Alpine compressional stresses - Alpine inversion - Late Cretaceous-Neogene inversion (The link with hyphen is misleading, since there were long pauses between events.)

Response -
We agree with the reviewer. Late Cretaceous shortening is expressed differently along the STZ via a number of different mechanisms. Within the Farsund Basin in particular, we show that this shortening is expressed via the reverse reactivation of normal faults (i.e. basin inversion), long wavelength folding of the basin fill and potentially regional uplift.
After the points raised and changes made in response to point 1 of the reviewer, we now use Late Cretaceous shortening/compression and Paleogene-Neogene uplift (Line 138) to refer to the two main events in this study. Within these overarching events, we are more explicit and refer directly to the different mechanisms, i.e. reverse fault reactivation etc., occurring along different parts of the northern basin margin.
As a result of these changes and an overall restructuring and clarification of the terms used in the manuscript, we have amended these "unclear relations" and "generalisations".

5. What is with in literature described indications of Paleogene uplift of this region?

Response
Because Uppermost Upper Cretaceous-Neogene strata are absent across the Farsund Basin, we are unable to distinguish individual Neogene and Paleogene uplift events, which we now refer to collectively as 'Paleogene-Neogene uplift,' (see responses above). We have clarified this in the revised manuscript (e.g. Line 154).
We have also included additional information relating to the potential causes of these uplift events (Line 146-152). Because strata and unconformities related to the Paleogene-Neogene

uplift event(s) are absent, we are unable to speculate as to the exact cause and timing of these uplift events, which we argue lie outside of the scope of this study.

6. a map of data coverage in relation to the interpreted structures would be useful

Response
A map of the seismic data referred to in this study is shown in Figure 8. We have also included the locations of the seismic sections and 3D seismic volume for the main study area on the revised Figure 2.

7. some questions of understanding to the data & methods chapter (see comments in the annotated PDF in the supplement). If possible, please make additional insertions in the text for better understanding.

Response
Specific points in response to comments raised in the annotated pdf are shown below.

8. line 448: Huyghe & Mugnier (1994, 1995) point to the relationship between rifting, the time elapsed thereafter and the potential for reactivation/inversion of the structure. So maybe the fault-reactivation and structural inversion with anticlinal folding is a consequence that compression in a properly aligned vector meets with the Farsund Basin a young "fresh" graben.

Response
We thank the reviewer for raising this interesting point regarding the young age of the Farsund Basin compared to other rift systems along the STZ. We agree that the short turnaround between extension and compression may increase the likelihood of reactivation within the Farsund Basin. Specifically, we note that the eastern segment of the Farsund North Fault, which formed only during Early Cretaceous rifting, may be more prone to reactivation than older structures.
We have incorporated some additional text discussing this idea, as proposed in Huyghe and Mugnier (1995), to lines 558-564. We also incorporate some additional information regarding the easterly rather than south-easterly trend of the Farsund Basin.

9. "488-490: We suggest that the likelihood of a structure to be reactivated and undergo inversion is not solely related to the size and ‘weakness’ of the structure; the relative complexity of the structure also plays an important role.“
Your presented seismic profiles show only the top 6 sec. twt of the strat. column. What information do the authors have about the geometry and complexity of the fault with the depth. A complex fault pattern in the most uppern strat. column does not have to mean that the fault in the deeper section must have a complex geometry.

Response
We agree that a complex fault pattern at shallow depths does not indicate a complex fault at depth. We are typically unable to identify any complex fault geometries at depth. We interpret that the Farsund North Fault is defined by a single planar fault geometry at depth.
We have amended the sentence in question to highlight that the along-strike complexity appears to represent the key aspect as to whether the structure was inverted (Line 336-338, 605)

10. Can statements about the amount of shortening during the Late Cretaceous and during "the Neogene" (if this event is related to shortening) be made?

Response
We are unable to comment on the absolute values of shortening that occurred during the Late Cretaceous. However, we do note that the amount of shortening was relatively mild and of a similar magnitude to that observed further west along the Stavanger Fault System, in the Egersund Basin (Line 517-518).
Well-based compaction analyses highlight the bulk amount of uplift that occurred in the immediate vicinity of the well, however, we are unable to distinguish between the distinct uplift events and phases that occurred. In response to earlier comments raised by the reviewer (see points 1 and 4) we have now changed the terminology used such that we no longer refer to "Neogene shortening" and instead refer to "Paleogene-Neogene uplift".

11. Various comments on illustrations (Please see the annotated PDF in the supplement). - Figure 3 and 11 in particular should be adapted.

Response
See specific responses below for each figure in response to the comments in the annotated pdf.

<u>Responses to annotated pdf comments – from supplement</u>
Minor textual changes and grammatical changes addressed in the pdf have been corrected in the revised manuscript and are shown in the attached track changes document, along with changes already made in response to the preceding points. We here list the more detailed changes made to the manuscript

12. Line 18 – "is it actually shortening or tilting or differential subsidence by other processes (e.g. dynamic topography?)
Response
We now refer to Paleogene-Neogene uplift as opposed to shortening. We are unable to comment directly on the cause of the uplift, although we do list some previously proposed mechanisms in Section 2.2.

13. Line 21 – Reactivation is perhaps the better umbrella term (rather than inversion), Inversion of faults, grabens, basins is not only the effect of upper cretaceous compression. In some areas only basement flexures and steep reverse faults along older permo-carboniferous pre-cursors can be seen (SE-Germany, NE-Germany). From this I would define structural inversion itself as a deformation-type-mechanism.

Response
We have modified this sentence so that it now reads "how compressional stresses may be accommodated by different mechanisms within structurally complex settings". We acknowledge that these compressional stresses and related basin shortening may be accommodated by different mechanisms. This is emphasised further in the revised Introduction (Line 30-34) and this terminology is applied throughout the manuscript

14. Line 32 – within the southe Permian Basin, structural inversion especially in the top of the Zechstein salt detachment shows often long-wavelength folding of the whole pre-inversion

structure “uberpresste Graben” (there exist no good translation, overpressed graben). Therefore some of the structures look a bit like positive flower structures (e.g. Kockel 2003). An effect of shortening of the post-Zechstein along a well-developed detachment.

Response
We agree with the reviewer that this represents an important potential mechanism of inversion. We have incorporated this mechanism and associated reference into the mechanism relating to the thin-skinned folding of strata above a detachment (Line 36).

15. Line 35-39 – most of the rift-structures or faults of the pre-Zechstein within the CEBS show steep dipping faults – sometimes near sub-vertical

Response
We agree that the majority of the faults in this area are steeply-dipping to sub-vertical. However, in this instance we are referring to pre-existing structures in general, and under which circumstances they may reactivate. We make no specific reference to the study area at this point in the manuscript.

16. Line 71, 120 –Comment regarding the (potentially earlier) onset of Neogene uplift

We agree with the reviewer that uplift did not solely occur in the Neogene, with earlier events occurring throughout the Paleogene. Following changes made in response to earlier comments we no longer refer to Neogene uplift and instead refer to Paleogene-Neogene uplift events (see responses to Points 2,4 and 5). We have modified the text in these areas to take this into account and added additional references where appropriate (Line 146-154).

17. Line 118 – From Jackson et al., 2013 – the inversion started in the latest Turonian and ceased in the Maastrichtian. More or less the same story as in the whole CEBS with main inversion from Santonian to Campanian. – Check the timing of the event from Jackson et al.

Response
We thank the reviewer for pointing this out. We have modified the date of inversion to that referred to in Jackson et al., (2013) (latest Turonian to Early Maastrichtian) (Line 143).

18. Line 125 – Map of the data coverage in relation to the interpreted fault segments would be useful

Response
We agree with this point raised by the reviewer and have since added the locations of the 2D seismic sections and 3D seismic volume used in this study to Figure 2, along with figure 8. This figure has also now been referenced accordingly in lines 161 and 165

19. Line 151 – This only minimises errors from the geometrical distortions of dipping structures in the time domain but not the error originating from the general increase in interval-velocities in most lithologies with depth. Therefore only the throw of faults in the same twt interval with more of less the same lithology would be comparable in the time domain.

Response
We agree with the reviewer that measuring throw as opposed to heave does not account for velocity distortions with depth. However, we primarily examine along-strike changes in fault

throw, where the lithologies in the hangingwall and footwall remain relatively constant along-strike. Furthermore, we do not focus on the absolute values of throw measured along the faults, rather the overall shape and distribution of throw along the faults. Therefore the changes in throw, which are less influenced by velocity distortions are key to our analysis, and underpin our related conclusions. We have added some text in the revised manuscript to address this point (Line 188-194)

20. Line 162 – Was decompaction taken into account in the course of calculating uplift?

Response
Decompaction was accounted for in the well-based calculations of uplift*. However, for the seismic-stratigraphic projections, we used a purely geometric approach and did not account for decompaction. The seismic-stratigraphic based approach is aimed at examining the spatial distribution of uplift across the basin rather than absolute values at specific points, as is the case for the well-based calculations. Although decompaction of the strata would change the magnitude of the uplift values calculated here, it would not change the overall spatial pattern. Using a seismic-stratigraphic based approach, we highlight that uplift increases across the basin to the north and to the east; we make no quantitative statements regarding the magnitude of uplift. Furthermore, decompaction would require a depth conversion of the data, which would incorporate more errors into our analyses (Lines 218-224).*

21. Line 175 – Was the effect of waterload considered wihtin the calculation? Along the Farsund Basin water depth reaches up to 500 m.b.s.l.

Response
The method used in this study only considers the loss of porosity resulting from the thickness of the overlying rock-column, which represents the major factor controlling porosity-loss due to mechanical compaction. Although the waterload will have an effect on the compaction of strata, we do not believe it to be a major factor (Line 247-248). Furthermore, our approach is consistent with previous studies of well-based uplift in this region (e.g. Japsen et al., 2007), which allows us to directly compare our estimates of uplift to these studies.

22. Line 189 – Mudstone is not just mudstone, there is a great variety of them. The decrease in porosity with depth can also show subtle correlations to, for example, palaeofacies, hydrostatic pressure conditions (Paleo/Recent), variance in mineral composition. In figure 6, a comparison between wells inside and outside the basin is shown. However the basin and the respective graben parts show strong activity especially during the lower cretaceous. How can other influences on the porosity distribution be excluded? A discussion or explanatory explanations would be nice.

Response
This is an interesting point raised by the reviewer. We agree that there is a large variability within mudstones and that other factors may play a role in the compaction of these strata with depth. The regional curve of Hansen et al, (1996) represents the average porosity-depth trend for Cretaceous-Tertiary shales across the Norwegian shelf, and as such likely smooths out these more local features.
We have added some additional text to the methods section highlighting how additional factors such as "mineralogy, paleogeographic setting, and burial rate" may affect local porosity-depth trends, but that these small-wavelength variations are largely smoothed out by the average trend of Hansen et al., (1996) (Line 255-258). We further address this point in the results section (Lines 363-366 in response to the reviewer comment on Line 286), where we suggest that the

scatter displayed by individual wells may relate to "minor lithological variations, possibly relating to subtle differences in palaeoenvironment and lithological/mineralogical changes between individual wells". The key point is, however, that overcompaction is present regionally in all wells.

23. Line 295, 313 – These estimates (seismic-stratigraphic projections or truncated strata) do not take into account compaction effects and is based only on the actual situation. Regardless of the fact that the analysis was performed in the time domain, the influence of sediment column compaction on the throw should be discussed.

Response
We agree that the absolute amplitude of the fold would likely increase following decompaction. Some text has been added to the revised manuscript discussing the effect of compaction on our uplift values in the methods section (Line 222-224).
Taking compaction into account, we would expect fold amplitude to decrease with depth due to increased compaction, the opposite to what we observe here, suggesting that decompaction has a limited effect and would only accentuate our current observations. The key point in this section is that fold amplitude changes, both with depth and along-strike, will largely be unaffected by decompaction. We have added text to this effect to the revised manuscript (Line 404-406)

24. Figure 5c – How do you define the base-level for calculation of fold-amplitude in each horizon? Do you see similar changes in the wave-length of the folding in to comparison to the other horizons? (the lateral effect of folding per horizon).

Response
Fold amplitude was measured between the fold crest and a local structural datum for each stratigraphic horizon. This local datum was taken as a projection of each stratigraphic horizon from an area unaffected by the near-fault folding. This has been made clearer in the revised manuscript (Line 200-202).

25. Line 351 – Provide references that refer to potential Carboniferous-Permian extension in the area

Response
Additional references have been added to this section, detailing Carboniferous-Permian extension occurring elsewhere along the Sorgenfrei-Tornquist Zone and also to the west in the Egersund Basin (Lines 442-445).

26. Line 357 – What kind of reactivation? Is it safe to assume that the entire fault plane has been reactivated?

Response
We have changed the phrasing of this section in the revised manuscript to state that the fault underwent "preferential reverse reactivation during Late Cretaceous compression" (Line 453). We assume in this instance that the fault plane was reactivated across all depths, although we are unable to determine whether this was the case, particularly across deeper structural levels.

27. Line 393 – "areas experienced less inversion and therefore preserve the initial monoclinal fold geometry" – What is meant in this context?

Response
The fault core and surrounding wall rocks have experienced more deformation and are possibly weaker than areas near the fault tips. As a result, weaker areas near the fault centre would be easier to invert when subject to compression. Thus, assuming the whole length of the fault was subject to the same compressional stress, the weak fault centre would reactivate more readily, and undergo reverse reactivation/slip and related folding of hangingwall strata (see Jackson et al., 2013). We have since altered the wording of this sentence to make this point clearer and relate to the relevant references (Line 489-492).

28. Line 395 – Please define your understanding of inversion/reactivation: Structural inversion related to faults, basin inversion, uplift/exhumation of basins, reactivation.

Response
See response to Points 1 and 4 above.

29. Line 395-396 – Can the Neogene uplift/exhumation really be explained by structural inversion? E.g. Kley (2018)
Response
See response to Points 1 and 4 above. We have added a reference to Kley, (2018) at this point, referring to the Paleogene uplift.

30. Line 402 – the mechanism behind Paleogene uplift/exhumation are under discussion. Refer to Kley et al., 2018

Response
This section refers to the compressional phase associated with Africa-Iberia-Europe convergence rather than the later Paleogene-Neogene uplift events. We have discussed the potential mechanisms behind Paleogene-Neogene uplift earlier in the manuscript (section 2.2).

31. Line 431-436 – See previous comments about Paleogene uplift and discuss further (e.g. line 395-396). Prominent refs include Kley et al., 2018

We have incorporated more information relating to Paleogene uplift at the start of section 6.2 and 2.2. However, as we are unable to distinguish between individual uplift events we do not go into detail as to the causes of each uplift event. In the sentence in question (now 536-538) we refer to the specific uplift of the South Scandes and South Swedish domes, which we interpret as the main reason for the spatial uplift patterns observed in the Farsund Basin (Lines 538-540). The Paleogene uplift referred to in Kley (2018), whilst being important at the regional scale and referenced accordingly in the Geological setting, is largely focussed south of the study area and does not concur with our spatial patterns of uplift.
We have removed a sentence corresponding to the regional uplift events and have clarified the sentence to make it clear that we are referring to the uplift of the domes to the north and east (Line 533-536).

32. Line 445 – it is obvious that the STZ localises over long time far-field stresses. The crucial question, however, is why there are so many different development histories along-strike of the STZ. Areas with an important Triassic-Jurassic history and others with Lower Cretaceous rifting and as well different degrees of Late Cretaceous deformation. On the other hand most the STZ

show an Upper Cretaceous shortening but to different degrees. Maybe the STZ reacts more sensitively to compression as to extension? Maybe the difference and the segmented characteristic is an effect of crustal heterogeneities along the STZ

Response
The reviewer raises an interesting point here. At upper crustal depths, the STZ is largely defined as a zone of Late Cretaceous shortening, with this shortening accommodated by a variety of mechanisms (e.g. reverse fault reactivation, long-wavelength folding of basin fill). We propose in this study that, at least at the basin-scale, the prior evolution of the basin plays an important role in how it accommodates these relatively far-field compressional stresses. The presence and prior evolution of the Farsund North Fault controls the structural style of shortening that occurs within the basin.
At the more regional scale, we agree with a previous comment raised by the reviewer that the young Early Cretaceous age of the graben, may influence how it behaves when subject to later compression. In accordance with that comment (addressed in Point 8), we have added some additional text to the revised manuscript stating the relatively young age of the Farsund Basin relative to other structures along the STZ may be more prone to reactivation (Huyghe and Mugnier, 1995) (Line 558-564).
During its history, the STZ has largely never been directly subject to either pure compression or extension, so we are unable to comment on whether it reacts more sensitively to one or the other. Instead the STZ typically reactivates via some component of oblique transtension/transpression (Japsen et al., 2007a; Mogensen, 1995). The style of this reactivation is, as the reviewer states, governed by the initial structure and segmented nature of the rift systems along the STZ. We highlight this for the Farsund Basin, and at a more local scale along its northern margin.

33. Line 480-482 – Are there any ideas what the mechanism behind this flexural/monoclinal bulge during the Neogene and the South Scandic Dome is? Dynamic topography? If the STZ will act as a hingeline for uplift during the Neogene facies distributional pattern of the Neogene should show similar trends. Are there any studies on this in regions with a more complete Neogene strat. Column? Your figures do not support the idea of the STZ as a hinge-line for uplift in the Neogene.

Response
Based on the regional nature of Paleogene-Neogene uplift, it has been proposed that this relates to a reorganisation of plate tectonic forces and also dynamic topographic effects relating to uplift of the South Scandes and South Swedish domes (Stoker et al., 2005, Japsen et al., 2007a, 2018, Kley et al., 2018). We have added some text to the revised manuscript in the geological history regarding these potential mechanisms (Lines 146-154, 536-537).
See also response to Points 2 and 5 above.
Because we do not see any preserved Upper Cretaceous-Neogene strata across the study area, we are unable to distinguish individual events and cannot identify any changes in depositional facies. However, based on the bulk uplift values calculated through our well analyses we suggest that the Sorgenfrei-Tornquist Zone represents a "relative" hingeline between areas experiencing large vertical motions to the north, and smaller vertical motions in the Norwegian-Danish Basin to the south. This is in agreement with previous studies in the area (Japsen et al., 2007a, 2018). We have modified the text to make our interpretation of a "relative" hingeline clearer in the revised manuscript (Line 594-596).

34. Line 490 – Your presented seismic profiles show only the top 6 s TWT of the strat column, what information do the authors have about the geometry and complexity of the fault with

depth? A complex fault pattern in the most upper strat column does not have to mean that the fault in the deeper section must have a complex geometry

Response
See response to Point 8 above.
Along the eastern segment of the fault, the area referred to as "relatively young and geometrically simple" (Line 561), we interpret a simple planar fault geometry at both shallow and deeper levels. We have since clarified this point in the conclusions to highlight that the along-strike changes in fault complexity are most important (Line 605).

35. Line 491-492 – The late cretaceous shortening is the result of far-field stresses. This means that more or less the whole STZ should have been affected by that in a similar way. Therefore, it would be strange if adjacent sections of the STZ would not show similar amounts of shortening or smoothed decreases or increases in a regional trend. In such cases there is a need for local additional effects (strain partitioning, transfer of shortening onto other structures, or a change in the deformation style).

Response
This is a good and interesting point raised by the reviewer. The Sorgenfrei-Tornquist Zone represents a buffer to inversion during the Late Cretaceous, and accordingly some shortening is observed along the whole of the structure in some form. Due to the regional and far-field nature of the applied stress, we would not expect any major changes in the amount of shortening experienced at the local scale. However we suggest that this shortening can be accommodated via different mechanisms along-strike, such that whilst the basin may experience changes in the degree of shortening via any one particular mechanism, the regional amount of shortening across the STZ remains relatively constant.
We observe relatively minor Late Cretaceous inversion along the Farsund North Fault; the magnitude of this inversion is similar to that observed along-strike to the west along the Stavnger Fault System in the Egersund Basin (Jackson et al., 2013). We have added some text to this effect in the revised manuscript (Line 517-518).

Figures

Figure 1 – Although a conceptual model, it would be good to highlight the stratigraphy of the region in the sketch

Response
We have incorporated some aspects of the Farsund Basin here (namely the colour scheme and unconformity) to enable comparison between this conceptual figure and the observed seismic sections, and also to highlight the difficulties presented in determining the age of the inversion along the fault due to the missing strata at the unconformity. However, this conceptual figure shows the geometry and formation of a typical inversion-related anticline, and is not intended to be specific to any particular lithologies. We believe that incorporating stratigraphic information into this figure will not add value.

Figure 2
Add co-ordinates
Altered in revised manuscript

Expand on what is meant by STZ projection

This has been changed on the figure to "Along-strike STZ continuation". This is based on projected continuations of the STZ to the west of the Farsund Basin.

Column labels too small in figure 1b. Enlarge section
The labels have been enlarged in this figure. In addition, some have been changed to reflect the content of the revised manuscript (i.e. Africa-Iberia-Europe Convergence).

Figure 3
At present-day – Are the faults really of Permo-Carboniferous age?
The majority of these faults only offset strata of proposed Carboniferous-Permian Age and show no offset at the base of the Zechstein. Therefore we suggest a likely Carboniferous-Permian age, in conjunction with previously documented Carboniferous-Permian rift activity in this area (see lines 430). However, we acknowledge that we cannot be certain of this age, and have amended the interpretation to state that the activity is pre-Zechstein, and likely Carboniferous-Permian.

Incomprehensible differences between interpretations of seismic section and the flattened seismic at End Triassic.

Why does the thickness of the brown pre-Zechstein unit change?
We are uncertain of the thickness of the brown pre-Zechstein unit as we have no direct constraints on the base horizon, which we represent by a dashed line. We have amended our interpretation of the unit to ensure compatibility between the two sections and to ensure that the thicknesses do not drastically change.

Why do faults with offsets on the base pre-Zechstein at the end of Triassic not show offsets in todays picture?
These faults have since been modified in the revised version of the figure.

Unusual changes in the distribution and interpretation of Zechstein
The interpretation of the Zechstein unit has been reinterpreted across both sections to ensure compatibility. Particular attention has been paid to the location of welds within the Zechstein and the salt structure on the right hand side of the section

Indications for Triassic offset on some faults?
Following a re-interpretation of the horizons across the flattened profile, we do not believe there to be any significant Triassic offset along the faults. E-W-oriented extension occurred during the Triassic, as documented in Phillips et al, (2018) and was accommodated along N-S-striking faults. We identify no activity along E-W striking faults during the Triassic, although some may offset the acoustic basement (base upper Permian) horizon, suggesting some relatively minor Permian activity.

Change in extent of Zechstein (i..e depositional limit)
This has now been amended in the revised version of the figure.

You have interpreted the Triassic picture in a way that no indications for pre-cursors of the STZ is given. Is this implication meant to be created, that the Farsund Basin coincides with the STZ, but does not show clear pre-Cretaceous pre-cursors?
This is intentional and is one of the interesting features of the Farsund Basin, namely that no clear evidence of Carboniferous-Permian extension is present, compared to elsewhere further east along the STZ. Prior to Early Cretaceous rifting, the Farsund Basin was located along the northern margin of the Norwegian-Danish Basin, with only some E-W-directed Triassic extension occurring in the area, producing N-S-striking faults. This figure highlights that, prior to Early

Cretaceous rifting, the Farsund Basin and Varnes Graben were continuous and resided along the northern margin of the Norwegian-Danish Basin.

Towards the NDB, you have interpreted a weld, but in the present-day section there is Zechstein again?
This has since been rectified in the revised version.

Top Zechstein is not consistent between figures at the large salt structure on the RHS
This has also been corrected in the revised version of the manuscript.

Figure 9 – Thinned layers on the central subfigure?
A label has been added to the central subfigure to indicate the thinning of strata across the fold. We suggest that this is a consequence of the earlier fault propagation folding that occurred during the Early Cretaceous extension.

Figure 11 –
shearing of pre-rift units along blind faults needs thinning of those units or additional minor faulting (in the fault propagation fold.
This has now been rectified on the revised figure to show thinning of the blue pre-rift interval across the fault within the fault propagation

Are there indication of decrease of normal thicknesses of pre-rift strata in the hangingwall of the main fault? Figure 9b indicates this, 9a and 9c do not.
There is no decrease in the thicknesses of the pre-rift strata across the main fault. An additional label has been added to the figure to make this clearer
.
The step from b to c is not fully comprehensible. If the onlap geometries and contact relations were as in sketch b before inversion, then inversion of the structure by reactivating the lower cretaceous main fault would result in a different picture. (rotaitons of the contacts of the lower cretaceous onlaps to peeusdo-downlaps. The actual thesis seems plausible, but its graphic implementation is not yet really coherent.

We have redrafted part c of this figure in order to make the geometric relations more apparent. We highlight that the onlapping geometries of the Lower Cretaceous strata would be rotated to form pseudo-downlaps and also highlight the variable fold amplitude with depth.

Pre-inversion normal fault geometry controls inversion style and magnitude, Farsund Basin, offshore southern Norway

Thomas B. Phillips[1], Christopher A-L. Jackson[2], James R. Norcliffe[2]

[1]Department of Earth Sciences, Durham University, Science Labs, Durham, DH1 3LE, UK
[2]Basins Research Group (BRG), Imperial College, London, SW7 2BP, UK

Correspondence to: Thomas B. Phillips (thomas.b.phillips@durham.ac.uk)

Abstract. ~~Inversion~~ Compressional stresses may localise along pre-existing structures within the lithosphere, far from the plate boundaries along which the causal stress is greatest. ~~Inversion~~ The style and magnitude of the related contraction is expressed in different ways, depending on the geometric and mechanical properties of the pre-existing structure. A three-dimensional approach is thus required to understand how ~~inversion~~ compression may be partitioned and expressed along structures in space and time. We here examine how ~~inversion~~post-rift compressional stresses ~~is expressed~~ manifest along the northern margin of the Farsund Basin during Late Cretaceous inversion and Paleogene-Neogene pulses of uplift. At the largest scale, ~~strain~~ stress localises along the lithosphere-scale Sorgenfrei-Tornquist Zone, where it~~; this~~ is expressed in the upper crust as hangingwall folding, reverse reactivation of the basin-bounding normal fault, and bulk regional uplift. The geometry of the northern margin of the basin varies along-strike, with a normal fault system passing eastward into an unfaulted ramp. Late Cretaceous compressive stresses, originating from the ~~Alpine Orogeny~~ convergence between Africa, Iberia and Europe ~~to the south~~, selectively reactivated geometrically simple, planar sections of the fault, producing hangingwall anticlines and causing long-wavelength folding of the basin fill. The amplitude of these anticlines decreases upwards due to tightening of pre-existing fault propagation folds at greater depths. In contrast, later –Paleogene-Neogene ~~shortening~~ uplift is accommodated by long-wavelength folding and regional uplift of the entire basin. Subcrop mapping below a major, ~~Neogene~~ uplift-related unconformity and borehole-based compaction analysis show that uplift increases to the north and east, with the Sorgenfrei-Tornquist Zone representing a hingeline ~~to inversion~~ rather than a focal point to uplift, as was the case during earlier ~~the~~ Late Cretaceous compression. We show how compressional stresses may be accommodated by different ~~inversion~~ mechanisms within structurally complex settings. Furthermore, the prior history of a structure may also influence the mechanism and structural style of ~~inversion~~ shortening that it experiences.

1 Introduction

Compressional stresses originating at plate boundaries can be transmitted great distances into continental interiors where they may localise along and drive ~~inversion~~ the reactivation and shortening of pre-existing lithospheric heterogeneities ~~in the lithosphere~~ (e.g. Berthelsen, 1998; Sandiford and Hand, 1998; Turner and Williams, 2004; Dyksterhuis and Müller, 2008;

Buiter et al., 2009; Stephenson et al., 2009; Heron et al., 2018). Inversion is intimately related to intra-plate compressional stresses, describing the process by which previously extensional structures are folded and/or uplifted (in the case of rift basins), or undergo reverse reactivation (in the case of a normal fault), in response to a change from an extensional to compressional tectonic stress (Cooper and Williams, 1989). In addition to long-wavelength folding of the basin fill (e.g. Liboriussen et al., 1987; Jensen and Schmidt., 1993), and reverse fault reactivation (e.g. McClay, 1995; Panien et al., 2006; Kelly et al., 2016; Reilly et al., 2017; Patruno et al., 2019; Rodriguez-Salgado et al., 2019; Scisciani et al., 2019), compressional stress may also be accommodated by additional mechanisms including: i) folding of strata atop a ductile detachment surface (e.g. Kockel, 2003); and ii)~~iii)~~ the formation of new reverse and strike-slip faults (e.g. Kelly et al., 1999; Rodriguez-Salgado et al., 2019). ~~Such inversion may be expressed via a range of mechanisms, including: i) (ductile) folding of strata (e.g. Jackson et al. 2013; Liboriussen et al., 1987; McClay, 1995~~Jackson et al. 2013;~~); ii) (brittle) reverse reactivation of previously extensional faults (e.g. Panien et al., 2006; Kelly et al., 2016; Reilly et al., 2017; Patruno et al., 2019; Rodriguez-Salgado et al., 2019; Scisciani et al., 2019); iii) the formation of new reverse and strike-slip faults (e.g. Kelly et al., 1999; Rodriguez-Salgado et al., 2019); and iv) regional basin uplift (Jensen and Schmidt., 1993).~~

The geometry and mechanical strength of pre-existing structures, and their relative position with respect to adjacent structures, may control if, to what extent, and how ~~these~~ different structures will be ~~inverted~~ behave when subject to compressional stresses (Kelly et al., 1999; Walsh et al., 2001; Panien et al., 2005; Reilly et al., 2017). According to Andersonian fault mechanics, low-angle structures are typically easier to reactivate under compression, whereas sub-vertical structures may be easier to reactivate in a strike-slip sense (Anderson, 1905; Daly et al., 1989). 'Weaker' structures, such as those characterised by high pore pressures and/or pervasive fabrics, are typically easier to reactivate than stronger, more homogeneous structures (Youash, 1969; Gontijo-Pascutti et al., 2010; Chattopadhyay and Chakra, 2013). Furthermore, certain structures may be preferentially reactivated, regardless of their strength, due to their location with respect to other structures, i.e. those located in the strain shadows of larger structures are unlikely to be reactivated (Walsh et al., 2001; Reilly et al., 2017). Once a structure does reactivate, our understanding of the structural styles and mechanisms of the associated ~~inversion~~ reactivation are typically thought of in only a 2D sense, with ~~reverse reactivated~~inverted normal faults producing relatively simple inversion-related anticlines (Fig. 1). Such an approach negates the inherent along-strike variability and prior evolution of ~~the inverted~~ structures, and thus leaves a number of unanswered questions. For example, (i) how does the prior evolution and geometry of a structure affect its propensity to ~~be inverted~~ reactivate ~~during~~ when subject to compression?; (ii) how does the style and magnitude of ~~inversion~~ this reactivation vary along-strike?; and (iii) how are different styles of ~~inversion~~deformation, (i.e. uplift, long-wavelength folding, reverse reactivation etc.) partitioned along-strike of a structure?~~.~~

We use borehole-constrained 2D and 3D seismic reflection data from the Farsund Basin, an inverted graben located offshore southern Norway, to examine how ~~compressional~~ compression and uplift-related stresses were partitioned between different styles and mechanisms of ~~inversion~~ deformation across a structurally complex rift basin (Fig. 2a). The Farsund Basin has experienced a complex and protracted geological evolution, being located above the westernmost extent of the lithosphere-scale, Sorgenfrei-Tornquist zone (STZ) (Fig. 2a). The STZ corresponds to a pronounced step in lithospheric thickness at sub-

crustal depths (e.g. Pegrum, 1984; Mogensen, 1994, 1995; Deeks and Thomas, 1995; Cotte and Pedersen, 2002; Babuška and Plomerová, 2004; Bergerat et al., 2007) and ~~was~~ has repeatedly reactivated in response to regional tectonic events, such as ~~(e.g.~~ Carboniferous-Permian transtension, Early Cretaceous extension, and Late Cretaceous ~~inversion~~ compression (Fig. 2b) (Mogensen 1995; Berthelsen 1998; Phillips et al. 2018). This multiphase and protracted evolution produced a complex rift system along its length, including the Farsund Basin. In addition, the~~Further deformation occurred in the~~ Farsund Basin area experienced further phases of uplift ~~in~~throughout the Paleogene and Neogene, ~~due to~~associated with regional uplift of southern Scandinavia (Japsen and Chalmers, 2000; Japsen et al., 2007a, 2018; Baig et al., 2019). This important tectonic event resulted in the formation of a large unconformity and the removal of large thicknesses of strata from across the basin (Fig. 1, 2b).

We focus on the northern margin of the Farsund Basin, which is defined by the complex S-dipping Farsund North Fault in the west and a S-dipping ramp to the east. (Fig. 2a). Specifically, using borehole-based compaction analyses, subcrop mapping, and qualitative (i.e. seismic-stratigraphic) and quantitative analysis of fault-related folds, we examine how ~~inversion~~ deformation was partitioned along this structure ~~throughout~~during ~~-~~Late Cretaceous compression and Paleogene-~~-~~Neogene ~~events~~ uplift events. Local r~~R~~everse reactivation of the basin-bounding Farsund North F~~f~~ault occurs locally and was associated with the formation of near-fault hangingwall anticlines and long-wavelength folding of the basin fill. The hangingwall anticline decreases in amplitude upwards; this is in contrast to the relatively constant amplitude~~at~~ typically encountered ~~in~~ along inversion-related folds. We suggest that this structural style is related to the presence of fault propagation folds formed along the fault prior to inversion. We find that reverse reactivation preferentially occurs along geometrically simple fault sections, areas that display a more complex fault geometry, or where rift-bounding faults are not present, are not reactivated and ~~inversion~~ shortening is largely manifest as regional uplift. We relate the reverse reactivation of the Farsund North Fault and the buckling of basin strata to ~~Alpine~~ compressional stresses associated with the convergence of Africa, Iberia and Europe during the Late Cretaceous, prior to the main Alpine orogeny (Kley and Voigt, 2008). This compression~~,~~ localised along and was~~ing and~~ buttressed against~~long~~ the lithosphere-scale STZ and, locally within the Farsund Basin, ~~particularly~~ the Farsund North Fault. We attribute the regional uplift and erosion to ~~Neogene~~ Cenozoic uplift of onshore Norway, with the STZ acting as a hingeline between areas of relative uplift and those of subsidence.

This study highlights how stresses associated with regional compression and uplift, initially localised along the lithospheric-scale STZ, may be expressed via different deformation mechanisms within complex ~~the~~ upper crustal rift systems. We show how the magnitude and style of ~~inversion~~compression- and uplift-related deformation can vary~~ies~~ along-strike of a single structure, depending on ~~the~~ its geometric complexity and prior~~e inversion evolution~~tectonic history.

2 Geological setting and evolution

The Farsund Basin, located ~50 km offshore southern Norway, is an E-trending Early Cretaceous graben that underwent ~~inversion~~ shortening and uplift during the Late Cretaceous ~~and~~ and throughout the Cenozoic~~Neogene~~ respectively (Jensen and Schmidt 1993; Mogensen 1995). The basin is defined by the N-dipping Fjerritslev Fault system along its southern margin and

the S-dipping Farsund North Fault along its northern margin (Phillips et al. 2018). The basin ~~can be~~is separated into an upper and lower terrace by a series of N-S-striking faults that also define the Varnes Graben, and the Eigerøy and Agder horsts to the north (Fig. 2a). East of the eastern termination of the Farsund North Fault and the Agder Horst, the northern margin of the Farsund Basin is represented by the S-dipping Agder Slope (Fig. 2a).

Detailed accounts of the structural and stratigraphic evolution of the Farsund Basin can be found in Phillips et al. (2018) and Phillips et al. (2019), respectively. We here outline the key phases in the pre-Late Cretaceous evolution of the basin~~pre-inversion tectonics~~, before detailing how the Late Cretaceous compression and later Paleogene-Neogene uplift ~~inversion ev~~events were expressed ~~in~~ across the basin and wider region.

2.1 Pre-~~inversion~~ Late Cretaceous evolution of the Farsund Basin

The Farsund Basin is situated towards the westernmost extent of the Sorgenfrei-Tornquist Zone, which forms the northwestern section of the lithosphere-scale Tornquist Zone (Pegrum, 1984; Berthelsen 1998; Thybo, 2000; Cotte and Pedersen 2002; Mazur et al. 2015). The Tornquist Zone represents a sharp change in lithospheric thickness and structure between thick cratonic lithosphere of the Eastern European Craton to the north and east, and younger, relatively thin lithosphere of central and western Europe to the southwest (e.g. Kind et al., 1997; Cotte and Pedersen, 2002; Babuška and Plomerová, 2004). At upper crustal depths, the Tornquist Zone has been periodically reactivated during multiple tectonic events and is described as a 'buffer zone' to regional tectonic stresses (Mogensen et al., 1995; Berthelsen, 1998).

T~~Carboniferous-Permian t~~ranstensional reactivation of the STZ during the Carboniferous-Permian was associated with rift activity and voluminous magmatism, including the emplacement of the WSW-trending Farsund Dyke Swarm (Fig. 2b) (Heeremans and Faleide, 2004; Heeremans et al., 2004; ; Wilson et al., 2004; Phillips et al., 2017; Malehmir et al., 2018). However, ~~no~~ no Carboniferous-Permian fault activity is identified in the Farsund Basin (Phillips et al., 2018), although some pre-upper Permian faulting, likely related to Carboniferous-Permian extension, ~~likely~~ occurred in the Norwegian-Danish and Egersund basins (Skjerven et al., 1983; Jackson and Lewis, 2013) (Fig. 2~~1~~, 3).

E-W oriented Triassic extension formed N-S-striking faults across the area, including those that internally dissect the Farsund Basin and those that bound the Varnes Graben (Fig. 2) (Vejbæk, 1990; Phillips et al., 2018). The fault defining the western margin of the Varnes Graben, and those internally dissecting the Farsund Basin, likely formed a single structure during the Triassic that bounded the eastern margin of the Stavanger Platform (Fig. 2a) (Phillips et al. 2018; 2019)~~. At this time, this structure bounded the eastern margin of the Stavanger Platform (Fig. 2a)~~. Upon their deposition, Triassic, and likely Jurassic strata were contiguous with those in the Varnes Graben to the north (Fig. 3). ~~During the Triassic,~~At this time, the proto-Farsund Basin resided along the northern margin of the Norwegian-Danish Basin, which continued northwards into the present Varnes Graben (Fig. 2, 3) (Phillips et al. 2019)~~. Upon their deposition, Triassic, and likely Jurassic strata were contiguous with those in the Varnes Graben to the north (Fig. 3).~~ During the Early-Middle Jurassic, ~~these~~ the N-S-striking fault~~s~~ along the eastern margin of the Stavanger Platform was~~ere~~ sinistrally offset by roughly E-W-striking strike-slip ~~activity~~faults.~~ along E-W striking faults~~. However, away from where they directly offset the N-S-striking faults (which act as piercing points in the

kinematic analysis of Phillips et al., 2018), the precise location and geometry of the strike-slip faults is unknown due to erosion at the Base Jurassic Unconformity (Phillips et al. 2018).

Dextral transtensional reactivation of the STZ occurred during the Early Cretaceous (Fig. 2b) (Mogensen, 1995; Erlström et al., 1997; Phillips et al., 2018). This was associated with the formation of the E-W-striking normal faults bounding the Farsund Basin, forming a graben and separating it from the Norwegian-Danish Basin (Fig. 2, 3). Early Cretaceous extension in the Farsund Basin was associated with relatively rapid slip on the basin-bounding faults and correspondingly high rates of basin subsidence and accommodation generation (Phillips et al., 2018). Sediment accumulation rates eventually outpaced accommodation generation and the faults were buried (Fig. 3). Cretaceous and younger strata are eroded across the study area below the Base Pleistocene Unconformity (Fig. 3).

2.2 Late Cretaceous compression and ~~Neogene~~Paleogene-Neogene uplift ~~inversion events~~

~~Late Cretaceous inversion~~ Compression and shortening, which was accommodated by a range of deformation mechanisms, occurred along the length of the Tornquist Zone due to ~~the~~ Late Cretaceous convergence between Africa, Iberia and Europe ~~Alpine-Carpathian orogeny to the south~~ (Fig. 2a) (e.g. Deeks and Thomas, 1995; Berthelsen, 1998; Hansen et al., 2000; Kley and Voigt, 2008). West of the Farsund Basin, mild inversion of~~along~~ the Stavanger Fault System occurred ~~during~~ from the ~~Santonian-Cenomanian~~latest Turonian to early Maastrichtian (Fig. 2a) (Jackson et al., 2013). Further fault inversion ~~Alpine inversion~~ is ~~also~~ documented elsewhere in the North Sea (Biddle and Rudolph, 1988; Cartwright, 1989; Jensen and Schmidt, 1993; Jackson et al., 2013).

Following Late Cretaceous compression, multiple phases of u~~U~~plift ~~and erosion also~~ occurred across southern Scandinavia and the North Sea throughout the Paleogene and ~~during the~~ Neogene (Clausen et al., 2000; Japsen et al., 2007a, 2018). As a result of this uplift, Cretaceous, Paleogene and Neogene strata are missing beneath the Base Pleistocene unconformity across much of the study area. These uplift events may be related to uplift of the South Swedish and South Scandes Domes across southern Scandinavia, likely as a result of upper mantle movements, and changing plate tectonic forces associated with opening of the North Atlantic (e.g. Jensen and Schmidt, 1993; Clausen et al., 2000, Japsen and Chalmers, 2000; Japsen et al., 2002, 2007a, 2018; Stoker et al., 2005; Kalani et al., 2015; Baig et al., 2019). Because Late Cretaceous-Neogene strata are missing across much of the study area, we do not distinguish between the distinct Post-Cretaceous uplift events, instead referring to them collectively as Paleogene-Neogene uplift.

~~due to uplift of the South Swedish and South Scandes domes and ridge push associated with the opening of the North Atlantic (Fig. 2b) (e.g. Jensen and Schmidt, 1993; Japsen and Chalmers, 2000; Japsen et al., 2002, 2018; Kalani et al., 2015; Baig et al., 2019).~~

3 Data and methods

3.1 Data

We use a 2D seismic reflection dataset covering the Farsund Basin. This dataset consists of 31 N-trending seismic sections tied by five E-trending sections (Fig. 2a). These data record to 7 seconds two-way-travel time (s TWT) and are closely-spaced (~3 km), allowing us to correlate our interpretations between individual sections. The seismic data are displayed as zero-phase and follow the SEG reverse polarity convention: a downward increase in acoustic impedance is represented by a trough (red) and a downward decrease in acoustic impedance is represented by a peak (black). The 2D seismic sections data were locally augmented by a 3D seismic volume providing coverage of the southern margin of the basin, which images to 4 s TWT (Fig. 2a).

The ages of mapped seismic horizons were constrained by well 11/5-1, located on the southern margin of the basin (Fig. 2a). Wells 9/3-1, 10/5-1, 10/7-1 and 11/9-1, located outside of the main study area, provided additional age constraints (Fig. 2a). Velocity log information from well 11/5-1, two additional wells within the STZ (J-1, Felicia-1), and four wells in the Norwegian Danish Basin (10/5-1, 10/8-1, F-1, K-1) were used to estimate the amount of uplift across the region (see Sect. 3.4.2). Due to incomplete coverage of the velocity log through the interval penetrated by 11/5-1, and in order to not introduce additional errors into our measurements, we did not depth convert the data. Well reports were also used to extract lithological information from each well in order to remove unsuitable lithologies from the porosity analyses.

3.2 Seismic interpretation

We mapped seven seismic horizons that define the present structure and allow us to constrain the temporal evolution of the study area (Fig. 3): i) Top crystalline basement, corresponding to the base of a Carboniferous-Permian aged interval; ii) top Acoustic Basement, corresponding to the base Upper Permian Zechstein Supergroup evaporites where present, and the base Triassic where the evaporites are absent; iii) the Base Jurassic Unconformity (BJU); iv) Top Jurassic; v) top Lower Cretaceous; vi) Top Cretaceous; and vii) the Base Pleistocene Unconformity. Additional horizons were interpreted within the Lower Cretaceous interval to help constrain the geometry and evolution of inversion-related structures.

3.3 Quantitative fault analyses

We calculated throw-length profiles along the Farsund North Fault to determine its kinematic evolution (e.g. Walsh et al., 2003; Duffy et al. 2015; Yielding et al. 2016). To accurately constrain the evolution of a fault we need to account for all slip-related strain, including both brittle faulting and ductile folding. Therefore, where necessary, such as in areas displaying complex fault geometries, or fault-parallel short-wavelength folding, we project horizon cutoffs onto the fault plane from a regional datum (Fig. 1) (e.g. Walsh et al. 1996; Long & Imber, 2012; Coleman et al. 2018). We minimise potential errors in our measurements by measuring ~~measure~~ fault throw as opposed to displacement, removing the potential for errors associated with depth conversion (Fig. 1). Some errors inevitably persist in our calculations, primarily relating to measurement error,

geometrical distortions originating from changing interval velocity with depth, and burial-related compaction of sedimentary strata. We find that the measurement errors are negligible and non-systematic, and therefore have a negligible effect on the overall throw distribution along faults. Errors associated with interval velocity changes and sediment compaction also have only a minor influence as lithologies do not drastically change along-strike of our throw-length plots. Furthermore, we focus on the overall throw patterns along the fault rather than specific values, with the former unaffected by any potential changes in interval velocity or compaction of the strata. We calculated throw-length plots for the Acoustic Basement, Base Jurassic Unconformity and Top Jurassic horizons, as these were almost fully preserved in both the hangingwall and footwall of the Farsund North Fault (Fig. 1). The Top Jurassic horizon is missing in the footwall of the fault in some areas due to erosion below the Base Pleistocene Unconformity; estimates of throw at this stratigraphic level therefore represents a minimum estimate. No Triassic strata are preserved on the upper terrace of the Farsund Basin (Fig. 2a); in these areas the Base Jurassic Unconformity forms a composite surface with the top Acoustic Basement. To quantify the magnitude of inversion experienced along the Farsund North Fault, we measured the amplitude of the fold, between the fold crest and a regional base-level, at multiple stratigraphic levels. The base-level was a projection of each stratigraphic horizon, taken from an area away from the fold and unaffected by folding.

~~Fold amplitude was measured from a regional datum unaffected by folding to the fold crest.~~

3.4 Quantifying uplift and erosion

3.4.1 Seismic-stratigraphic analysis

To estimate the amount of uplift and erosion that occurred along the northern margin of the Farsund Basin, truncated stratigraphic horizons were projected above the Base Pleistocene Unconformity. By approximating their pre-erosion stratigraphic thickness, we can estimate the amount of missing strata and therefore erosion that occurred across the basin (Fig. 4). The top of the Cromer Knoll Group (Lower Cretaceous) represents the shallowest mapped horizon that is truncated by the Base Pleistocene Unconformity. This horizon is interpreted as the base of the syn-inversion sequence along the Stavanger Fault System, 100 km to the west (Fig. 2a) (Jackson et al., 2013). The deepest regionally mappable horizon truncated by the Base Pleistocene Unconformity is typically the Acoustic Basement. We measure uplift between the projections of these horizons, with the measurement taken at the truncation of the deeper horizon. However, in some areas we measure uplift at the Farsund North Fault to avoid assumptions about projected stratal thicknesses across the fault (Fig. 4). As a result, our seismic-stratigraphic technique provides only a minimum estimate of the amount of uplift. We provide two measurements of (minimum) inversion-related uplift along the basin margin by: (1) projecting strata linearly from the immediate subcrop; and (2) modifying the subcrop projections to take into account regional thickness changes within the underlying stratigraphic intervals (Fig. 4). These uplift calculations are based solely on geometrical projections of truncated strata and do not incorporate any decompaction of the projected strata. Upon burial sedimentary strata are compacted; layers are thus thinner at their present burial depths than they were when deposited. Therefore, our uplift estimates based on the geometric projection

of 'compacted' sedimentary intervals, which is based on their buried rather than at-surface thicknesses, represent a minimum value only. We primarily use this technique to analyse the spatial distribution of uplift across the Farsund Basin in locations where no boreholes are available and where we therefore lack information on the present porosity of the intervals at depth. Although the estimated *magnitude* would change upon decompaction, the overall *pattern* of uplift will not be affected.

3.4.2 Well-based compaction analysis

In addition to using seismic-stratigraphic techniques to estimate inversion-related basin-scale uplift, we also utilise porosity-depth trends and compaction analyses from seven wells within and surrounding the Farsund Basin (Fig. 2a). This process is based on the recognition that due to mechanical compaction and diagenesis, sedimentary rocks lose porosity (ø) with increasing burial depth (z) (Magara, 1978; Sclater and Christie, 1980). This porosity loss is largely inelastic (Giles et al, 1998), meaning that if a rock is uplifted it will be overcompacted relative to its new depth of burial (Magara, 1978; Japsen, 1998; Japsen et al., 2007a). The net magnitude of vertical exhumation (E_N) can hence be calculated by subtracting the porosity measured at present-day burial depth ($B_{present\text{-}day}$) from the maximum depth of burial (B_{max}) (Corcoran and Doré, 2005):

$$E_N = B_{max} - B_{present\text{-}day} \quad (1)$$

B_{max} is commonly predicted from porosity-depth relationships calibrated in settings characterised by continuous subsidence and progressive burial (Jensen and Schmidt, 1993; Doré and Jensen, 1996; Williams et al, 2005; Burns et al, 2007; Japsen et al 2007a; Tassone et al, 2014). Whilst such trends have been generated for discrete lithologies (e.g. Sclater and Christie, 1980), it is more accurate to use regionally calibrated relationships for specific stratigraphic intervals (Japsen et al, 2007b).

Here, we use porosity-depth data to estimate the exhumation of Lower Cretaceous mudstone and to quantify the magnitude of inversion-related basin-scale uplift. We used the Lower Cretaceous interval because it is the only mudstone-bearing interval encountered in all seven wells, where it varies in vertical thickness from 105-615 m. Six of these wells (10/8-1, 10/5-1, K1, F1, J1 and Felicia-1) were included in previous regional studies of basin exhumation, although different stratigraphic intervals (i.e. Late Cretaceous chalks) were used in these previous analyses (Japsen and Bidstrup, 1999; Japsen et al., 2007a). Well 11/5-1, which is located on the south flank of the Farsund Basin (Fig. 2a), has not previously been used for exhumation analysis and thus provides new constraints on inversion-related regional uplift of the Farsund Basin. No overpressure is identified in the Lower Cretaceous interval across any of the wells analysed in this study, hence they are assumed to be hydrostatic; this is in agreement with other studies in the region (e.g. Japsen et al., 1998). In keeping with previous well-based studies of compaction in the region, we do not account for compaction due to the water column.

Two porosity-depth relationships have been proposed for Norwegian Shelf Cretaceous-Tertiary shales (Hansen, 1996), one linear and one exponential:

$$ø = 0.62 - 0.00018z \quad (2)$$

$$ø = 0.71e^{(-0.00051z)} \quad (3)$$

These relations represent the *average* Tertiary-Lower Cretaceous porosity-depth trend; scatter in the original dataset may relate to variations in grain size and the proportion of shale in the lithological column. Aside from compaction, local porosity-depth trends may also be affected by the mineralogy, paleogeographic setting, and burial rate of the shales. In order to compare wells from different regions, we compare to this average porosity-depth trend, which largely smooths out these more local effects. Although both trends were derived statistically from porosity-depth data from 29 wells from areas that have not been uplifted (Hansen, 1996), we use the exponential relationship because it better conforms to rock physics models in that it does not predict negative porosities at depths greater than 3444 m, as is the case for the linear trend (Japsen et al., 2007b).

To compare well-log data to regional predictions of B_{max}, slowness values (Δt, measured in μs/ft), measured by the sonic log, were converted into porosities using a regionally calibrated modification (Hansen, 1996) of the Wyllie-time average equation (Wyllie et al., 1956):

$$\emptyset=(1/1.57)((\Delta t-59)/(189-59)) \quad (4)$$

Given that this relationship is valid only for shales, sonic log readings within intra-Lower Cretaceous sandstone and limestone beds were identified (via the well report) and removed from the analysis, anomalous reading were likewise removed. ~~Given that this relationship is valid only for shales, intra-Lower Cretaceous sandstone and limestone beds were identified (via the well report) and removed from the analysis.~~ Intra-shale porosities were then averaged over 5 m intervals and plotted against the depth (below the seabed) mid-point for this interval.

Following log editing and porosity estimations, we calculated net exhumation (E_N) (Eq. 1) for each porosity-depth datapoint from each well. These E_N estimates were then averaged to produce one exhumation estimate per well. Across the Farsund Basin, the Base Pleistocene unconformity is overlain by ~100-200 m of sediments (~156 m in 11/5-1) (Fig. 3). This indicates that any exhumation recorded by the Lower Cretaceous shales has been followed by further burial. If not properly accounted for, this post-uplift burial (B_E) will obscure porosity-derived exhumation estimates. The following equation (Corcoran and Doré, 2005) was used to derive the gross exhumation (E_G) from the net exhumation (E_N):

$$E_G= E_N+B_E \quad (5)$$

In each well, B_E was assumed to equal the vertical thickness of supra-Base Pleistocene unconformity sediments. Our borehole-based compaction analyses provide spot measurements of uplift in the Farsund Basin and surrounding areas. We combined these results with those derived from the seismic-stratigraphic techniques described above, allowing us to determine how uplift varied spatially across the area.

4 Structural style variability along the northern margin of the Farsund Basin

The structural style of the northern margin of the Farsund Basin varies along-strike (Fig. 5a). Early-Middle Jurassic strike-slip activity resulted in across-fault juxtaposition of different structural elements (i.e. the hangingwalls and footwalls of N-S striking faults), which were then extensionally offset by the Farsund North Fault during the Early Cretaceous (Phillips et al. 2018). Based on the structural elements in the hangingwall and footwall of the fault, we define four structural domains along the northern margin of the basin (Fig. 5a): A) the western end of the Farsund North Fault, with the Eigerøy Horst in the footwall and the upper terrace of the Farsund Basin in the hangingwall; B) a structurally complex zone along the Farsund North Fault with the Varnes Graben in the footwall and the upper terrace of the Farsund Basin in the hangingwall; C) the eastern end of the Farsund North Fault, with the Varnes Graben in the footwall and the lower terrace of the Farsund Basin in the hangingwall; and D) east of the Farsund North Fault, incorporating the eastern termination of the fault, with the Agder Horst in its footwall, and the Agder slope further east.

4.1 Domain A – Reactivation of an older fault?

No Triassic strata are present in Domain A due to erosion at the Base Jurassic Unconformity (Fig. 5a). Throw across the equivalent Acoustic Basement and Base Jurassic Unconformity horizons reaches a maximum of ~~is~~ ~1000 ms TWT in the centre of the domain. ~~, whereas the minimum~~ Tthrow across the top Jurassic horizon is ~500 ms TWT, reaching a maximum of ~600 ms TWT, although we~~;~~ note this represents~~is~~ a minimum throw estimate due to erosion of Jurassic strata across the Eigerøy Horst in the footwall of the Farsund North Fault (Fig. 5a). ~~Earlier,~~Early-Middle Jurassic strike-slip activity, ~~likely Carboniferous-Permian activity may have~~ likely occurred along the fault in this area, although we are unable to determine the geometry of the strike-slip fault system~~is~~ due to erosion at the Base Jurassic Unconformity (Phillips et al., 2018) (Fig. 5a). Earlier pre-Zechstein fault activity may also have occurred in this area, similar to that identified to the west in the Egersund Basin (Jackson and Lewis, 2013), although we are unable to confirm this. We identify a clinoform bearing interval in the upper Jurassic, likely related to the Farsund Delta system identified by Phillips et al. (2019). ~~This delta continues northwards into the Varnes Graben, suggesting a relatively young (i.e. post-Late Jurassic and, we suggest, Early Cretaceous) age for uplift of the Eigerøy Horst and corresponding slip on the Farsund North Fault.~~ F~~We identify f~~urther clinoform-bearing intervals are present in~~in~~ the Early Cretaceous succession; these may be locally sourced from erosion of the Eigerøy Horst. The Farsund North Fault and Lower Cretaceous strata in its immediate hangingwall are truncated by the Base Pleistocene Unconformity ~~close to the fault~~, indicating they have experienced some uplift. The lack of major hangingwall deformation suggests that the Farsund North Fault in this area experienced little to no reverse reactivation (Fig. 5a).

4.2 Domain B – Complex strike-slip related faulting

Domain B is characterised by a complex zone of faulting consisting of a main central fault that is flanked by numerous antithetic and synthetic faults (Fig. 5a). Triassic strata are preserved in the footwall (i.e. the Varnes Graben), but eroded from

the hangingwall (see Phillips et al., 2018). In contrast, Jurassic strata are continuous across the fault. Throw is constant (~500 ms TWT) across the fault for all horizons (Fig. 5b). Cretaceous strata thicken from the footwall to hangingwall of the fault and are truncated at the overlying Base Pleistocene Unconformity. Phillips et al. (2018) estimate this domain experienced ~10 km of sinistral strike-slip offset during the Early-Middle Jurassic, based on the offset of N-S striking fault, WVG, which bounds the western margin of the Varnes Graben, and the N-S-striking fault, NS1, which partitions the Farsund Basin to the south (Phillips et al., 2018). We suggest that ~~T~~the proposed strike-slip fault continues westwards, along the present location of the Farsund North Fault, ~~towards~~ in Domain A ~~A to the west~~. Further east, the Farsund North Fault shows only Early Cretaceous extensional activity, with no strike-slip precursor present along the fault in Domain C. Therefore, we suggest that the strike-slip fault~~, and continues to the~~ continues in a NW-SE orientation~~southeast~~, to the south of the Farsund North Fault (Fig. 5a) ~~Domain C, to the east~~. Phillips et al., (2018) document a similar relationship along the southern margin of the Farsund Basin, where the strike-slip fault system is proposed to continue in a NW-SE orientation to the north of an Early Cretaceous fault segment, displaying a complementary relationship to that proposed here along the northern margin. T~~Based on t~~he truncation of Lower Cretaceous strata beneath the Base Pleistocene Unconformity in Domain B suggest that some~~, inversion may have caused~~ uplift and erosion has occurred~~compression and uplift of Domain B, although this is difficult to determine~~.

4.3 Domain C – Reverse reactivation and hangingwall folding

Triassic and Jurassic strata are isochronous and display relatively constant throw across Domain C (Fig. 5a, b). Throw increases from ~600 ms TWT in the west to a maximum of ~1100ms TWT in the centre, before decreasing to ~800 ms TWT at the boundary with the Agder Horst to the east (Fig. 5b). Unlike Domain B, we suggest that this area did not experience any Early-Middle Jurassic strike-slip faulting, with the ~~proposed~~ strike-slip fault, collocated with the Farsund North Fault in Domain B to the west, continuing to the southeast, south of the Farsund North Fault, in ~~this area~~Domain C (Phillips et al., 2018). The Farsund North Fault in this area ~~is represented by~~ forms a planar~~straight~~ structure that slipped only during the Early Cretaceous (Fig. 5a). Some antithetic faults in the hangingwall merge with the main ~~structure~~ fault plane at depth. A large anticline is present in the hangingwall of the Farsund North Fault in Domain C, the amplitude of which is greatest at the top of the Jurassic and decreases ~~towards shallower levels (~~upwards (Fig. 5c). The amplitude of the fold also decreases towards the edges of Domain C, suggesting it ~~has~~ is a periclin~~eal geometry~~. Lower Cretaceous strata are truncated by the Base Pleistocene Unconformity and are not preserved on the footwall of the fault. Based on the stratigraphic relationships outlined above, ~~-w~~We suggest that Domain C represents an Early Cretaceous segment of the Farsund North Fault~~, which propagated away from a pre-existing segment (Domain A) during the Early Cretaceous~~. The throw maxima along the Farsund North Fault in Domains A and C suggest that the fault is formed of two linked segments separated by the complex deformation zone and strike-slip faulting within Domain B. We suggest that Domain C propagated away from the pre-existing strike-slip fault and this area of complex deformation (Domain B) during the Early Cretaceous, forming a new fault segment.~~, with Domain B situated between the two segments.~~

4.4 Domain D – Basin uplift and erosion

Domain D is largely characterised by the S-dipping Agder Horst, which hosts numerous low-displacement, E-W-striking, N-dipping faults. At the western end of the domain, ~~T~~ the Farsund North Fault terminates eastwards into numerous S-dipping splays; further eastwards propagation of the fault was~~,~~ potentially inhibited by~~due to the presence of~~ the basement-hosted Farsund Dyke Swarm (Fig. 5a) (Phillips et al., 2017). Strata are progressively truncated northwards at the Base Pleistocene Unconformity, indicating ~~wholesale~~ long-wavelength basin-scale uplift and erosion (Fig. 5a).

5 Styles of inversion

5.1 Regional uplift and erosion

Strata along the northern margin of the Farsund Basin are variably truncated at the Base Pleistocene Unconformity. We here use compaction analyses and seismic-stratigraphic methods to quantify the amount and patterns of ~~inversion-related~~ uplift driving this erosion.

5.1.1 Well-based compaction analyses

We plotted porosity-depth data from seven wells against the Lower Cretaceous compaction curve of Hansen (1996). This normal compaction curve, which assumes continuous burial and hydrostatic stress conditions, lies below data from each all of the wells (Fig. 6a), indicating that overcompaction is present regionally. Porosity-depth data from each well show significant scatter, which is likely a result of minor lithological variations, possibly relating to temporal changes in palaeoenvironment. There are also likely to be lithological and mineralogical changes between wells. However, we interpret the regional and ubiquitous presence of overcompaction relative to the baseline to determine the magnitude of exhumation.

Porosity-depth data cluster in two depth-intervals (170-825 m and 1080-1460 m depth; Fig. 6a). The shallower cluster contains data from wells 11/5-1, Felicia-1 and J1, all of which are located within the STZ (Fig. 2a). These wells record gross-exhumation values 647-775 m, with 11/5-1 recording the greatest amount of exhumation (775 m) (Fig. 6b). The deeper cluster contains data from wells 10/5-1, 10/8-1, F-1 and K-1; all of which are situated south of the Farsund Basin and STZ (Fig. 2a). Importantly, ~~E~~exhumation estimates from these wells are overall lower than those to the north, varying from 273-683 m. Well 10/5-1, which is located closest to the STZ, records the highest gross exhumation (683 m), whereas wells 10/8-1, F-1 and K-1 record values of 270 m, 405 m, and 295 m respectively (Fig. 6b). In summary, our analyses show that the amount of exhumation increases towards the STZ (Fig. 2a); no well information is available ~~further~~ north of the STZ.

5.1.2 Seismic-stratigraphic analyses

By projecting strata as a straight line based on the dip at the point they are truncated beneath the Base Pleistocene Unconformity, we estimate ~100 ms TWT uplift in Domain A, increasing to a maximum of ~400 ms TWT in Domain C. this

value then decreases to ~250 ms TWT across the Agder Slope (Fig. 5c). Our other technique which varies the dip of the projected strata to account for underlying stratal geometries, suggests ~200 ms TWT of uplift in Domain A increasing to ~400 ms TWT in Domains B and C these values are thus similar to those obtained using a straight projection method. Corrected projection measurements predict ~800 ms TWT in Domain D (Fig. 5c). Here, the straight projection method underestimates uplift as truncated strata become more steeply south-dipping to the north. Older strata progressively subcrop the Base Pleistocene Unconformity towards the north and east (Fig. 7, 8). Acoustic Basement subcrops the Base Pleistocene Unconformity on the Eigerøy and Agder horsts, due to their location in the footwalls of the bounding faults of the Varnes Graben. The ages of strata subcropping the Base Pleistocene Unconformity also increases northwards across the Agder Slope. Jurassic and Lower Cretaceous strata subcrop the Base Pleistocene Unconformity in the Varnes Graben (Fig. 8). The increase in erosion to the north and east, combined with the projections of truncated strata, together suggest that the magnitude of the causal uplift increases in these directions. ~~This suggests an increase in uplift to the north. Across the Farsund Basin, uplift~~ Uplift ~~-~~particularly increases eastwards~~, particularly~~ past the eastern termination of the Farsund North Fault (Domain D). As ~~N~~no fault is present here,~~reverse reactivation of the fault occurs in this area (see below) and bulk~~long-wavelength, regional uplift appears to represent the main mechanism accommodating ~~inversion related~~ shortening in this domain (Fig. 7). ~~Older strata progressively subcrop the Base Pleistocene Unconformity towards the north and east (Fig. 7, 8). Acoustic Basement strata subcrop the Base Pleistocene Unconformity on the Eigerøy and Agder horsts, due to their location in the footwalls of the bounding faults of the Varnes Graben. Deep strata also subcrop the Base Pleistocene Unconformity further east along the Agder Slope. Jurassic and Lower Cretaceous strata subcrop the Base Pleistocene Unconformity in the Varnes Graben (Fig. 8).~~

5.2 Evidence for fault reactivation

A prominent hangingwall anticline occurs in Domain C of the Farsund North Fault (Fig. 5a, 9). The fold incorporates Upper Triassic to Lower Cretaceous strata, before it is truncated upwards by the Base Pleistocene Unconformity (Fig. 9). The fold is ~35 km long, extending from the westernmost part of Domain B in the west and terminating to the east next to the Agder Horst in Domain D (Fig. 5a, c). The amplitude of the fold is greatest in the middle of Domain C (~200 ms TWT), decreasing to zero at its lateral terminations. The amplitude of the fold varies with depth; it is similar at Top Jurassic and Base Jurassic Unconformity levels (~150 ms TWT), decreasing upwards into the Lower Cretaceous (~80 ms TWT) (Fig. 5c). The fold is typically tightest close to or just above the top of the Jurassic ~~interval~~, where it is often deformed by normal faults along its hinge (Fig. 9a). Although the absolute fold amplitude will be affected by compaction of strata, we suggest that this will not alter how the amplitude changes along-strike and with depth, i.e. that fold amplitude is greatest at the centre of the fold and at greater depths. Lower Cretaceous strata thin by up to 50% onto the hangingwall-facing limb of the fold, and often onlap onto this limb at deeper levels (Fig. 9b, c).

Stratigraphic thinning and onlap onto fault parallel hangingwall folds are characteristic of extensional growth folds (also known as ‘fault-propagation folds’ or ‘forced folds’; see review by Coleman et al., 2019). These folds, which are initially expressed as basinward-facing monoclines, typically form above the propagating upper tiplines of blind normal faults (Mitra and Islam,

1994). These folds are subsequently breached during subsequent fault slip and tip propagation. However, in the Farsund Basin, the fault-parallel fold is anticlinal as opposed to monoclinal, suggesting that this is not the cause of the folding. Anticlinal fault-parallel hangingwall folds may form as fault-bend folds due to changes in fault dip (e.g. Suppe, 1983; Withjack and Schlische, 2006). However, we discount such an origin here due to the relatively planarity of the fault and lack of major dip changes (Fig. 9).

Based on the observations outlined above, we interpret the fault-parallel hangingwall fold as an inversion-related anticline (e.g. Dart et al., 1995; Lowell, 1995; Turner and Williams, 2004; Yamada and McClay, 2004). No null point is identified along the fault, with all horizons displaying net extension, indicating the magnitude of the initial extension was much greater than the subsequent inversion. Due to erosion at the Base Pleistocene Unconformity, the crest of the fold and any associated growth strata are not preserved, providing no direct constraints on the timing of fold formation or causal inversion (Fig. 1, 9). However, the folding (and inversion) must have occurred post-Early Cretaceous, given Lower Cretaceous strata are incorporated in the fold (Fig. 9).

We also identify a minor graben in the centre of the Farsund Basin, bound by faults that span a depth range of ~1000 ms TWT in the thickest part of the Lower Cretaceous syn-rift succession (Fig. 10). These faults are basement detached, terminating downwards at ~1500 ms TWT and upwards, either within the upper levels of the Lower Cretaceous interval or by truncation at the Base Pleistocene Unconformity (Fig. 10). They are associated with relatively low displacements (~10-20 ms TWT) that are greater at shallower levels (~20 ms TWT). At depth, fault displacements are typically below seismic resolution but the faults can be identified by clear fault plane reflections (Fig. 10).

We interpret these structures as outer-arc flexural faults formed in response to basin compression and related hangingwall buckling (e.g. Panien et al., 2005, 2006). The decrease in throw with depth suggests arching of the basin fill, whilst their relatively uniform termination depth may define the fold neutral surface, with areas above under extension, and below under overall compression (Fig. 10). A ~65 ms TWT thick clinoform-bearing interval is present at ~750 ms TWT in the Lower Cretaceous interval, prograding basinwards from the southern margin of the basin (Fig. 10). The presence of basinwards prograding clinoforms indicate that the basin still represented a depocentre at that time.

6 Discussion

6.1 Structural styles and expression of inversion

Inversion-induced hangingwall folding only occurs locally along the eastern segment of the Farsund North Fault (Domain C), with little direct evidence for reverse reactivation being observed elsewhere (Fig. 5a). The fault in Domain B is characterised by a complex zone of faulting formed during Early-Middle Jurassic strike-slip faulting (Phillips et al., 2018); this domain is located between two segments of the Farsund North Fault of potentially differing ages (Fig. 5a). The eastern fault segment (Domain C) only initiated in the Early Cretaceous, with Carboniferous-Permian strata being isopachous across the fault (Fig. 3). The western segment of the Farsund North Fault (Domains A and B) was also active during Early Cretaceous extension,

~~and~~ may have been active as a strike-slip structure during the~~earlier during~~ Early-Middle Jurassic (Phillips et al., 2018) and, potentially, as a normal fault during the~~-~~ Carboniferous-Permian ~~extension~~activity along the Sorgenfrei-Tornquist Zone (e.g. Skjerven et al., 1983; Mogensen, 1994; Erlström et al., 1997).~~,~~ However, we~~ although we~~ are unable to confirm this due to a lack of preserved strata (Fig. 5a). Similarly, along the southern margin of the Farsund Basin, the ~~southern strand of the Fjerritslev Fault System~~Fjerritslev South Fault was inactive prior to the Early Cretaceous extension, at which time it propagated westwards from a pre-existing ~~-~~segment of the fault that had previously experienced strike-slip motion (Fig. 2a) (Phillips et al., 2018). We also suggest that the Farsund North Fault propagated eastwards in the Early Cretaceous from an area where a pre-existing, previously strike-slip fault segment was present (Domains A and B). The eastern segment (Domain C) thus represents the youngest, and accordingly the least complex, section of the Farsund North Fault, forming a simple planar structure (Fig. 9). We suggest that the relatively simple geometry of the eastern segment of the Farsund North Fault caused it to undergo~~be~~ preferential~~ly~~ reverse reactivation~~ed~~ during Late Cretaceous compression~~inversion~~. Whilst other sections of the fault may have been weaker, they were not reactivated due to their more complex geometry, related to their prior evolution and segmentation. Similar links are made between highly deformed and complex fabrics within shear zones (such as those typified by recumbent and isoclinal folding); in these settings, ~~and~~ the lack of major fault exploitation during subsequent extension ~~as~~ reflects the complexity of the shear zone fabric, which may inhibit ~~blocks~~ lateral fault propagation (Morley, 1995; Salomon et al., 2015). Along the Farsund North Fault, local stress field interactions between different structures and fault segments may result in an obscuring of any pervasive anisotropy, inhibiting strain localisation and therefore reactivation.

Typically, during reverse reactivation, pre-inversion strata in the hangingwall of the fault are folded into an inversion-related anticline of constant amplitude with depth (Fig. 1) (Mitra and Islam, 1994; Lowell, 1995; McClay, 1995). However, observations of the eastern segment of the Farsund North Fault (Domain C) diverge from this, with fold amplitude decreasing towards shallow depths (Fig. 5c, 9). Some of this decrease in amplitude may be attributed to the interplay between the folding of competent and incompetent units in the fold core~~ of the fold~~. More competent units will deform via folding and maintain a constant thickness, whereas less competent units will not maintain thickness and may be extruded from the core of the fold. The increased compaction of deeper buried strata would result in a potential decrease in fold amplitude with depth, the opposite to that observed in the Farsund Basin (Fig. 5c). The Lower Cretaceous interval comprises relatively homogeneous siltstones, with no major changes in lithology and competency expected. Although lithologies do vary within the Jurassic interval (Phillips et al., 2019), this does not correlate to the location of the change in fold amplitude (Fig. 9). Furthermore, the magnitude of the amplitude change is likely too large to be explained by the mechanical properties of the strata alone.

Along the Farsund North Fault, strata within the lower sections of the Lower Cretaceous interval onlap folded strata within the inversion anticline and thin onto the hangingwall limb of the fold (Fig. 9). These stratal relationships suggest some relief at the free surface in the hangingwall of the Farsund North Fault during Early Cretaceous ~~extension and fault slip~~faulting. Fault propagation folding of Jurassic and Early Cretaceous strata occurs along the southern margin of the Farsund Basin, associated with Early Cretaceous faulting (Phillips et al., 2018); we suggest that the Farsund North Fault may have experienced similar fault-propagation folding during Early Cretaceous extension.

Based on the variable fold amplitude and stratal relationships within the hangingwall of the Farsund North Fault, we propose the following model to explain ~~its inversion and~~ the ~~resultant~~ structural style of the inversion-related anticline. The eastern segment of the Farsund North Fault (Domain C) formed as a new structure, propagating eastwards away from the pre-existing strike-slip fault during Early Cretaceous extension (Fig. 2a, 5a). This extension was associated with fault propagation folding of Jurassic and lowermost Lower Cretaceous strata; the fault propagation fold~~, which~~ was subsequently breached and buried ~~by~~ within the uppermost Lower Cretaceous succession (Fig. 11a, b). During ~~inversion~~Late Cretaceous compression, folding of near-fault strata within the upper parts of the Lower Cretaceous succession produced a ~60 ms TWT amplitude inversion-related anticline in the immediate hangingwall of the fault ~~anticline~~ (Fig. 5c, 12c). However, at deeper structural levels, where pre-inversion strata were already folded, the initial monoclinal fold was tightened and rotated, forming a higher amplitude~~n~~ inversion-related anticline (Fig. 12c). The amplitude of the resultant composite fold at depth thus reflects both the Early Cretaceous fault propagation folding and the subsequent Late Cretaceous ~~subsequent~~ inversion, similar to ~~those~~ fold structures produced by Mitra and Islam (1994). Towards the lateral terminations of the fold, at the boundaries of Domain C, we observe a more monoclinal fold geometry (Fig. 9c). We speculate that the centre of the fault is likely weaker than the fault tips and therefore easier to reactivate under compression (Reilly et al., 2017; Rodriguez-Salgado et al., 2019). As a result, the fault tips typically experience less reverse reactivation than in the fault centre, thus preserving more of the earlier~~, as these areas experienced less inversion and therefore preserve the initial~~ monoclinal fold geometry in the former location.

6.2 Temporal and spatial partitioning of inversion styles

The Farsund Basin experienced ~~at least two phases of inversion~~a period of shortening during the Late Cretaceous followed by~~and~~ pulses of regional uplift throughout the Cenozoic, largely during the Paleogene and Neogene (Hansen et al., 2000; Gemmer et al., 2002; Kalani et al., 2015; Kley, 2018). During these events, ~~the~~ various deformation mechanisms ~~accommodating inversion~~ were spatially partitioned across the Farsund Basin; regional uplift occurred ~~along the northern margin of the basin~~across the whole of the northern basin margin (Fig. 7), the Farsund North Fault underwent local reverse reactivation (Fig. 9), ~~whereas~~ and the basin fill was buckled into an open long-wavelength anticline (Fig. 10). Due to truncation of syn-inversion strata at the Base Pleistocene Unconformity, we cannot directly assign these different ~~inversion~~ mechanisms to the Late Cretaceous or Paleogene-Neogene events.

Late Cretaceous ~~inversion~~ compression is related to convergence between~~the Alpine Carpathian Orogeny~~ Africa, Iberia and Europe, with three distinct ~~tectonic~~ compressional pulses recognised in the Danish area during the Late Cretaceous and Paleogene (Kley and Voigt, 2008; Hansen et al., 2000; Gemmer et al., 2002). Within the upper crust, the STZ is defined by a zone of Late Cretaceous ~~inversion~~ shortening (e.g. Pegrum, 1984; Liboriussen et al., 1987; Michelsen and Nielsen, 1993; Mogensen and Jensen, 1994; Deeks and Thomas, 1995; Mogensen, 1995; Lamarche et al., 2003; Bergerat et al., 2007). Along the Tornquist Zone, Late Cretaceous inversion is expressed via numerous mechanisms, including reverse fault reactivation (Kryzwiec, 2002), transpression (Deeks and Thomas, 1995), and basin-scale compression and uplift (Liboriussen et al., 1987; Erlström et al., 1997; Hansen et al., 2000). Late Cretaceous inversion has also been observed westwards along-strike of the

STZ in the Egersund Basin (Pegrum, 1984; Sørensen et al., 1992; Phillips et al., 2016), where inversion ~~along~~ of the Stavanger Fault System initiated during the Coniacian (~86.3 Ma) to Santonian (~82.6 Ma) and continued until the Maastrichtian (~66 Ma) (Jackson et al. 2013). Inversion was relatively mild in the Egersund Basin, producing inversion-related folds of 300-450 m amplitude (Jackson et al., 2013). In comparison, the degree of inversion accommodated by hangingwall folding ~~within the Farsund Basin~~along the Farsund North Fault produces an inversion anticline that has an amplitude of ~80 ms TWT at shallower depths. We suggest the amplitude of the fold at shallow depths is more representative of the structural style forming during Late Cretaceous ~~Neogene inversion~~ shortening, with the amplitude of the fold at greater depths accentuated by earlier fault propagation folding (Fig. 11, see above). Comparison with inversion along the Stavanger Fault System in the adjacent Egersund Basin suggests that the Farsund Basin also experienced mild shortening during the Late Cretaceous. Some components of inversion within the Farsund Basin may also be partitioned into regional uplift and long-wavelength folding of the basin fill, as well as the reverse reactivation of the previously extensional normal faults and associated hangingwall folding. Based on similarities in the magnitude and style of inversion between the Farsund and Egersund basins, we suggest that the reverse reactivation of the Farsund North Fault likely occurred during the Late Cretaceous. Long-wavelength folding of the basin fill, the ~~and~~ formation of outer-arc flexural faults within the basin, and the formation of Tornquist Zone-adjacent Late Cretaceous depocentres resembles the long-wavelength folding and basin inversion ~~and the formation of Tornquist Zone-adjacent Late Cretaceous depocentres~~ observed elsewhere along the Tornquist Zone (Fig. 10) (Liboriussen et al., 1987; Japsen et al., 2002), also suggesting this deformation is Late Cretaceous. At this time, the Farsund North Fault acted as a buttress to Late Cretaceous compression, undergoing reverse reactivation and folding in the immediate hangingwall with simultaneous long-wavelength folding and uplift of the basin fill (Fig. 12a).

As well as reverse fault reactivation and long-wavelength folding of the basin fill, the entire northern margin of the Farsund Basin was uplifted, as is evident from subcrop projections (Fig. 7). In contrast to Late Cretaceous compression, this uplift is not buttressed by the Farsund North Fault, increasing north and east towards the Norwegian mainland and across the Agder Slope (Fig. 5c). Some of this uplift may be attributed to Late Cretaceous compression, although we are unable to distinguish between this and later uplift~~e two events~~ due to a lack of preserved post-Late Cretaceous strata (Fig. 7). ~~Strata are tilted and truncated along the eastern margin of the North Sea rift towards the Norwegian mainland, related to the onset of North Atlantic rifting and potential magmatic underplating (Japsen, 1998; Japsen and Chalmers, 2000; Gemmer et al., 2002; Baig et al., 2019).~~ Offshore southern Norway, Paleogene-Neogene uplift ~~is specifically~~has been proposed to be related to the uplift of the South Scandes Dome beneath southern Norway to the north, exposing Proterozoic basement onshore, and uplift of the South Swedish Dome beneath Southern Scandinavia to the east (Jensen and Schmidt, 1992; Japsen et al., 2002). The distribution of these domes is consistent with observations of uplift from the Egersund Basin (Kalani et al., 2015) and our observations of the increase in uplift to the north and east being related to the South Scandes and South Swedish domes respectively.

6.3 Localisation of inversion along pre-existing structures

The STZ may act as a weak buffer zone to regional tectonic stresses, effectively shielding the cratonic lithosphere of the Eastern European Craton to the north and east (e.g. Berthelsen, 1998; Hansen et al., 2000; Mogensen and Korstgård 2003). During Late Cretaceous ~~inversion~~compression, the pronounced change in lithospheric thickness and properties across the zone localises far-field stresses originating from the south associated with the ~~Alpine Orogeny~~convergence between Africa, Iberia and Europe (Fig. 12a) (Kley and Voigt, 2008). Such long-lived and lithosphere-scale structures, upon which strain can localise, are lacking in the relatively young lithosphere beneath Central and Western Europe and the North Sea (Pharaoh, 1999). How this compression localises along various parts of the STZ is largely governed by the structural style and pre-existing rift physiography present.

Numerical modelling has highlighted that deformation will localise along weak lithosphere-scale structures, such as the STZ (Gemmer et al., 2002). Far-field stresses focus along heterogeneities situated at great depths or spanning large depth ranges within the lithosphere. Structures within the mantle lithosphere can control the location of rifting in extensional settings (i.e. the Davis Strait in the Labrador Sea) and orogenic belts in compressional settings (i.e. the Ouachita Orogeny, USA) (Heron et al., 2018, 2019). Rift basins may also form crustal-scale heterogeneities prone to inversion, even long after extension stops. Weaknesses developed at mid-crustal depths during rift-related crustal necking, or irregularities along the Moho, may prime rift systems for later inversion (Hansen and Nielsen, 2003; Buiter et al., 2009). Crustal-scale faults, such as those bounding the Farsund Basin, also weaken the lithosphere and increase the likelihood of basin and fault inversion during subsequent regional compression (Lie and Husebye, 1994; Hansen and Nielsen, 2003; Phillips et al., 2018). The relatively young, Early Cretaceous, age of the Farsund Basin, and the relatively short time between Early Cretaceous extension and Late Cretaceous inversion, may also increase its propensity to be inverted when subject to compression (Huyghe and Mugnier, 1995). Specifically, the relatively young eastern segment of the Farsund North Fault, which initiated as a new fault during the Early Cretaceous, may have been more prone to reverse reactivation when subject to subsequent compression (Huyghe and Mugnier, 1995). Furthermore, the easterly trend of the Farsund North Fault, compared to the typical NW trend observed elsewhere along the STZ, may have been more optimally oriented for reactivation when subject to Late Cretaceous compression.

At the crustal scale, inversion preferentially occurs on larger structures that are typically weaker, having experienced more deformation (Reilly et al., 2017). The geometry and relative location of fault segments and systems within a larger fault array, as opposed to the inherent strength of the fault itself, forms a primary control on whether, and to what extent a structure will reactivate (Walsh et al., 2001; Reilly et al. 2017). Optimally-located structures tend to increasingly localise strain, growing larger at the expense of smaller structures residing in ‘strain shadows’, which ultimately become inactive. The larger, typically more continuous structures are preferentially reactivated in later events. Although areas of the Farsund North Fault may have experienced more deformation and be weaker than other areas, they often display a more complex geometry than newly formed structures. For example, the eastern segment of the Farsund North Fault represented a single structure that formed a focal point for Late Cretaceous ~~inversion~~compression and underwent inversion; faults bounding the southern margin of the Farsund Basin

were not inverted. The southwards dip of the Farsund North Fault, coupled with its crustal-scale geometry and location along the northern boundary of the STZ buttress, mean the fault was ideally situated to accommodate Late Cretaceous ~~inversion-related~~ compressional stresses and undergo reverse reactivation (Fig. 12a).

Whilst the STZ and the Farsund North Fault localise stresses during Late Cretaceous ~~inversion~~compression, this is not apparent during Paleogene-Neogene uplift (Fig. 12). Uplift increases regionally from zero in the Norwegian-Danish Basin south of the study area, to 1000 m across the Skagerrak-Kattegat Platform to the northeast (Japsen et al., 2002). Based on basin modelling and regional borehole-based porosity analyses of Upper Cretaceous chalks, Japsen et al., (2002) propose 600-800m uplift along the STZ, consistent with our estimation of 775m uplift in the Farsund Basin, based on borehole-based porosity analysis of the Lower Cretaceo~~o~~e~~o~~us interval penetrated in well 11/5-1. These values are also consistent with our estimates of uplift from the Felicia-1 (640 m) and J-1 (655 m) boreholes located further eastwards along the STZ. Uplift decreases southwards away from the STZ to around ~300 m within the Norwegian-Danish Basin. Relatively high uplift values (~400m) are documented in the F-1 well (Fig. 2a), although this may in part relate to local salt mobilisation (Fig. 3). The regional south-north uplift gradient drastically increases at the STZ, as evidenced by the two clusters of uplift estimates from nearby wells; those wells situated atop the STZ, typically experience 600-800m uplift whereas those further the south document only ~300m (Fig. 2a, 6a). Uplift within the STZ may be locally augmented by Late Cretaceous uplift related to fault reactivation and localised hangingwall uplift; however, as the uplift increases away from the STZ and the Farsund North Fault to the north and east, we suggest that any pre-~~Neogene~~ Cenozoic (i.e. Late Cretaceous) uplift contributes only a negligible amount of uplift to the regional values. Locally, within the Farsund Basin, uplift increases northwards away from the STZ (Fig. 12b). To the east, where uplift also increases, the STZ rotates to strike NW-SE, such that east of Domain D may be located north of the STZ and uplift again increases. Rather than localising deformation as it does ~~during~~ in response to Late Cretaceous ~~inversion~~compression, we suggest that the STZ represents a relative hingeline ~~to uplift during the Neogene~~throughout the Paleogene and Neogene uplift events (Fig. 12b), modulating and partitioning vertical motions in the Norwegian-Danish Basin to the south, from those larger motions occurring to the north, supporting the interpretation of previous regional studies (Japsen et al., 2007a; 2018).

7 Conclusions

In this study, we show how ~~inversion~~ deformation may be ~~is~~ expressed along a complex pre-existing structure via various ~~different~~ mechanisms ~~throughout~~ during Late Cretaceous shortening and Paleogene-Neogene ~~compressional~~uplift events. Late Cretaceous compression was accommodated via selective reverse reactivation of the Farsund North Fault, forming a prominent hangingwall anticline. This reactivation occurred along the relatively young and geometrically simple eastern segment of the fault, which propagated from a pre-existing structure during Early Cretaceous extension. We suggest that the likelihood of a structure to be reactivated and undergo inversion is not solely related to the size and 'weakness' of the structure; the relative complexity of the structure also plays an important role. We find that the geometrically simple areas of the Farsund North Fault are preferentially inverted, whereas ~~those~~ areas along-strike with a more complex geometry that experienced~~,~~

~~likely having experienced~~ a more protracted evolution, typically do not localise strain and are not inverted. Late Cretaceous compression was also expressed as long-wavelength folding of the basin fill, buttressed against the Farsund North Fault, resulting in basin~~-scale~~ inversion and uplift and erosion.

We find that the geometry and prior evolution of a structure also influences the structural style of the resultant inversion-related structures. The presence of an extensional fault propagation fold, formed prior to inversion, along the Farsund North Fault results in the formation of an inversion-related hangingwall anticline that decreases in amplitude upwards~~ during inversion~~. Fold amplitude at shallow depths reflects the inversion event and reverse reactivation of the fault, whereas fold amplitude at depth reflects both inversion-related and earlier fault propagation folding.

Following Late Cretaceous compression, ~~During the Neogene,~~ the Farsund Basin experienced widespread uplift throughout the Paleogene and Neogene related to uplift onshore Norway and Sweden. Based on borehole-based porosity analyses within the Farsund Basin and surrounding area, we find that uplift increased to the north and east of the basin, with relatively smaller amounts of uplift occurring in the Norwegian-Danish Basin to the south. To the east of the basin, ~~W~~where the Farsund North Fault was not present, this represents the only mechanism of ~~inversion~~ uplift expressed in the basin.

Late Cretaceous compression localised along the lithosphere-scale STZ; in contrast, ~~ Neogene~~ stresses associated with Paleogene-Neogene uplift were not localised along the STZ, with the STZ instead~~ appearing to~~ representing a relative hinge-line~~ during this time~~, separating areas of low uplift to the south, from relatively large amounts of uplift further north.

The Farsund North Fault along the northern margin of the STZ acted as a buttress to compression within the upper crust, with inversion expressed as reverse reactivation, long-wavelength hangingwall folding and regional basin-scale uplift. At upper crustal depths, the prior evolution and geometric complexity of a pre-existing structure plays an important role in how and to what extent that structure may be reactivated during late compression.

Data availability: The seismic data used throughout this study are publically available for download via the DISKOS online portal (https://portal.diskos.cgg.com).

Author Contributions: TP is the primary author on this study, responsible for the interpretation and writing of the manuscript. CALJ contributed to the genesis of the manuscript and the writing and editing of the manuscript. JN carried out to the borehole-based compaction analyses and contributed to the writing and editing of the manuscript.

Competing interests: The authors declare that there are no competing interests.

Acknowledgements: This research is funded by a Leverhulme Trust Early Career Fellowship (ECF-2018-645) awarded to Phillips. The authors thank Schlumberger for providing academic licences to Durham University and Imperial College for use

of the Petrel Software. The authors would also like to thank Pablo Rodriguez-Salgado and Fabian Jähne-Klingberg for their constructive and detailed reviews that greatly improved the manuscript.

References

Anderson, E.M., 1905. The dynamics of faulting. Transactions of the Edinburgh Geological Society 8, 387-402.

Babuška, V., Plomerová, J., 2004. The Sorgenfrei–Tornquist Zone as the mantle edge of Baltica lithosphere: new evidence from three-dimensional seismic anisotropy. Terra Nova 16, 243-249.

Baig, I., Faleide, J.I., Mondol, N.H., Jahren, J., 2019. Burial and exhumation history controls on shale compaction and thermal maturity along the Norwegian North Sea basin margin areas. Marine and Petroleum Geology 104, 61-85.

Bell, R.E., Jackson, C.A.L., Whipp, P.S., Clements, B., 2014. Strain migration during multiphase extension: Observations from the northern North Sea. Tectonics 33, 1936-1963.

Bergerat, F., Angelier, J., Andreasson, P.-G., 2007. Evolution of paleostress fields and brittle deformation of the Tornquist Zone in Scania (Sweden) during Permo-Mesozoic and Cenozoic times. Tectonophysics 444, 93-110.

Berthelsen, A., 1998. The Tornquist Zone northwest of the Carpathians: An intraplate pseudosuture. Gff 120, 223-230.

Biddle, K.T., Rudolph, K.W., 1988. Early Tertiary structural inversion in the Stord Basin, Norwegian North Sea. Journal of the Geological Society 145, 603-611.

Buiter, S.J.H., Pfiffner, O.A., Beaumont, C., 2009. Inversion of extensional sedimentary basins: A numerical evaluation of the localisation of shortening. Earth and Planetary Science Letters 288, 492-504.

Burns, W.M., Hayba, D.O., Rowan, E.L., Houseknecht, D.W., Haeussler, P., Galloway, J., 2005. Estimating the amount of eroded section in a partially exhumed basin from geophysical well logs: an example from the North Slope. US Geological Survey professional paper, 1-18.

Cartwright, J.A., 1989. The kinematics of inversion in the Danish Central Graben. Geological Society, London, Special Publications 44, 153-175.

Chattopadhyay, A., Chakra, M., 2013. Influence of pre-existing pervasive fabrics on fault patterns during orthogonal and oblique rifting: an experimental approach. Mar. Pet. Geol. 39, 74-91.

Clausen, O.R., Nielsen, O.B., Huuse, M. & Michelsen, O., 2000. Geological indications for Palaeogene uplift in the eastern North Sea Basin. Global and Planetary Change, 24, 175-187.

Coleman, A.J., Duffy, O.B., Jackson, C.A.L., 2019. Growth folds above propagating normal faults. Earth-Science Reviews 196, 102885.

Corcoran, D., Doré, A., 2005. A review of techniques for the estimation of magnitude and timing of exhumation in offshore basins. Earth-Science Reviews 72, 129-168.

Cotte, N., Pedersen, H.A., 2002. Sharp contrast in lithospheric structure across the Sorgenfrei–Tornquist Zone as inferred by Rayleigh wave analysis of TOR1 project data. Tectonophysics 360, 75-88.

Daly, M.C., Chorowicz, J., Fairhead, J.D., 1989. Rift basin evolution in Africa: the influence of reactivated steep basement shear zones. Geological Society, London, Special Publications 44, 309.

Dart, C.J., McClay, K., Hollings, P.N., 1995. 3D analysis of inverted extensional fault systems, southern Bristol Channel basin, UK. Geological Society, London, Special Publications 88, 393.

Deeks, N.R., Thomas, S.A., 1995. Basin inversion in a strike-slip regime: the Tornquist Zone, Southern Baltic Sea. Geological Society, London, Special Publications 88, 319.

Doré, A.G., Jensen, L.N., 1996. The impact of late Cenozoic uplift and erosion on hydrocarbon exploration: offshore Norway and some other uplifted basins. Global and Planetary Change 12, 415-436.

Duffy, O.B., Gawthorpe, R.L., Docherty, M., Brocklehurst, S.H., 2013. Mobile evaporite controls on the structural style and evolution of rift basins: Danish Central Graben, North Sea. Basin Res 25, 310-330.

Dyksterhuis, S., Müller, R.D., 2008. Cause and evolution of intraplate orogeny in Australia. Geology 36, 495-498.

Erlström, M., Thomas, S.A., Deeks, N., Sivhed, U., 1997. Structure and tectonic evolution of the Tornquist Zone and adjacent sedimentary basins in Scania and the southern Baltic Sea area. Tectonophysics 271, 191-215.

Gemmer, L., Huuse, M., Clausen, O.R., Nielsen, S.B., 2002. Mid-Palaeocene palaeogeography of the eastern North Sea basin: integrating geological evidence and 3D geodynamic modelling. Basin Res 14, 329-346.

Gontijo-Pascutti, A., Bezerra, F.H.R., La Terra, E., Almeida, J.C.H., 2010. Brittle reactivation of mylonitic fabric and the origin of the Cenozoic Rio Santana Graben, southeastern Brazil. J. S. Am. Earth Sci. 29, 522-536.

Giles, M., Indrelid, S., James, D., 1998. Compaction—the great unknown in basin modelling. Geological Society, London, Special Publications 141, 15-43.

Hansen, D.L., Nielsen, S.B., 2003. Why rifts invert in compression. Tectonophysics 373, 5-24.

Hansen, D.L., Nielsen, S.B., Lykke-Andersen, H., 2000. The post-Triassic evolution of the Sorgenfrei–Tornquist Zone — results from thermo-mechanical modelling. Tectonophysics 328, 245-267.

Hansen, S., 1996. A compaction trend for Cretaceous and Tertiary shales on the Norwegian shelf based on sonic transit times. Petroleum Geoscience 2, 159-166.

Heeremans, M., Faleide, J.I., 2004. Late Carboniferous-Permian tectonics and magmatic activity in the Skagerrak, Kattegat and the North Sea. Geological Society, London, Special Publications 223, 157-176.

Heeremans, M., Faleide, J.I., Larsen, B.T., 2004. Late Carboniferous -Permian of NW Europe: an introduction to a new regional map. Geol Soc London, Special Publication 223, 75-88.

Heron, P.J., Peace, A.L., McCaffrey, K., Welford, J.K., Wilson, R., van Hunen, J., Pysklywec, R.N., 2019. Segmentation of rifts through structural inheritance: Creation of the Davis Strait. Tectonics 0.

Heron, P.J., Pysklywec, R.N., Stephenson, R., van Hunen, J., 2018. Deformation driven by deep and distant structures: Influence of a mantle lithosphere suture in the Ouachita orogeny, southeastern United States. Geology 47, 147-150.

Huyghe, P. & Mugnier, J.L. 1995. A comparison of inverted basins of the Southern North Sea and inverted structures of the external Alps. In: Buchanan, J.G. & Buchanan, P.G. (Eds.): Basin Inversion. Vol. 88: pp. 339-353; London, Geological Society Special Publication.

Jackson, C.A.L., Chua, S.T., Bell, R.E., Magee, C., 2013. Structural style and early stage growth of inversion structures: 3D seismic insights from the Egersund Basin, offshore Norway. Journal of Structural Geology 46, 167-185.

Jackson, C.A.L., Lewis, M.M., 2013. Physiography of the NE margin of the Permian Salt Basin: new insights from 3D seismic reflection data. J. Geol. Soc. 170, 857-860.

Japsen, P., 1998. Regional velocity-depth anomalies, North Sea Chalk; a record of overpressure and Neogene uplift and erosion. AAPG Bulletin 82, 2031-2074.

Japsen, P., Bidstrup, T., 1999. Quantification of late Cenozoic erosion in Denmark based on sonic data and basin modelling. Bulletin of the Geological Society of Denmark 46, 79-99.

Japsen, P., Bidstrup, T., Lidmar-Bergström, K., 2002. Neogene uplift and erosion of southern Scandinavia induced by the rise of the South Swedish Dome. Geological Society, London, Special Publications 196, 183.

Japsen, P., Chalmers, J.A., 2000. Neogene uplift and tectonics around the North Atlantic: overview. Global and Planetary Change 24, 165-173.

Japsen, P., Green, P.F., Chalmers, J.A., Bonow, J.M., 2018. Mountains of southernmost Norway: uplifted Miocene peneplains and re-exposed Mesozoic surfaces. Journal of the Geological Society 175, 721.

Japsen, P., Green, P.F., Nielsen, L.H., Rasmussen, E.S., Bidstrup, T., 2007a. Mesozoic–Cenozoic exhumation events in the eastern North Sea Basin: a multi-disciplinary study based on palaeothermal, palaeoburial, stratigraphic and seismic data. Basin Res 19, 451-490.

Japsen, P., Mukerji, T., Mavko, G., 2007b. Constraints on velocity-depth trends from rock physics models. Geophysical Prospecting 55, 135-154.

Jarsve, E.M., Maast, T.E., Gabrielsen, R.H., Faleide, J.I., Nystuen, J.P., Sassier, C., 2014. Seismic stratigraphic subdivision of the Triassic succession in the Central North Sea; integrating seismic reflection and well data. Journal of the Geological Society 171, 353.

Jensen, L., Schmidt, B., 1992. Late Tertiary uplift and erosion in the Skagerrak area: magnitude and consequences. Norsk Geologisk Tidsskrift 72, 275-279.

Jensen, L., Schmidt, B., 1993. Neogene uplift and erosion offshore south Norway: magnitude and consequences for hydrocarbon exploration in the Farsund Basin, Generation, accumulation and production of Europe's hydrocarbons III. Springer, pp. 79-88.

Kalani, M., Jahren, J., Mondol, N.H., Faleide, J.I., 2015. Compaction processes and rock properties in uplifted clay dominated units– the Egersund Basin, Norwegian North Sea. Marine and Petroleum Geology 68, 596-613.

Kelly, P., Peacock, D., Sanderson, D., McGurk, A., 1999. Selective reverse-reactivation of normal faults, and deformation around reverse-reactivated faults in the Mesozoic of the Somerset coast. Journal of Structural Geology 21, 493-509.

Kind, R., Gregersen, S., Hanka, W., Bock, G., 1997. Seismological evidence for a very sharp Sorgenfrei-Tornquist Zone in southern Sweden. Geological Magazine 134, 591-595.

Kley, J., Voigt, T., 2008. Late Cretaceous intraplate thrusting in central Europe: Effect of Africa-Iberia-Europe convergence, not Alpine collision. *Geology* ; 36 (11): 839–842. doi: https://doi.org/10.1130/G24930A.1

Kley, J., 2018. Timing and spatial patterns of Cretaceous and Cenozoic inversion in the Southern Permian Basin. Geological Society, London, Special Publications, 469, 19-31. https://doi.org/10.1144/SP469.12.

Kockel, F., 2003. Inversion structures in Central Europe – Expressions and reasons, an open discussion. Geologie en Mijnbouw. Netherlands Journal of Geosciences, 82, 4: pp. 367-382.

Liboriussen, J., Ashton, P., Tygesen, T., 1987. The tectonic evolution of the Fennoscandian Border Zone in Denmark. Tectonophysics 137, 21-29.

Lie, J., Husebye, E., 1994. Simple-shear deformation of the Skagerrak lithosphere during the formation of the Oslo Rift. Tectonophysics 232, 133-141.

Lowell, J.D., 1995. Mechanics of basin inversion from worldwide examples. Geological Society, London, Special Publications 88, 39.

Magara, K., 1979. Thickness of Removed Sedimentary Rocks, Paleopore Pressure, and Paleotemperature, Southwestern Part of Western Canada Basin1: DISCUSSION. AAPG Bulletin 63, 814-815.

Malehmir, A., Bergman, B., Andersson, B., Sturk, R., Johansson, M., 2018. Seismic imaging of dyke swarms within the Sorgenfrei–Tornquist Zone (Sweden) and implications for thermal energy storage. Solid Earth 9, 1469-1485.

Mazur, S., Mikolajczak, M., Krzywiec, P., Malinowski, M., Buffenmyer, V., Lewandowski, M., 2015. Is the Teisseyre-Tornquist Zone an ancient plate boundary of Baltica? Tectonics 34, 2465-2477.

McClay, K.R., 1995. The geometries and kinematics of inverted fault systems: a review of analogue model studies. Geological Society, London, Special Publications 88, 97.

Michelsen, O., Nielsen, L.H., 1993. Structural development of the Fennoscandian border zone, offshore Denmark. Marine and petroleum geology 10, 124-134.

Mitra, S., Islam, Q.T., 1994. Experimental (clay) models of inversion structures. Tectonophysics 230, 211-222.

Mogensen, T., Jensen, L., 1994. Cretaceous subsidence and inversion along the Tornquist Zone from Kattegat to the Egersund Basin. First Break 12, 211-222.

Mogensen, T.E., 1994. Palaeozoic structural development along the Tornquist Zone, Kattegat area, Denmark. Tectonophysics 240, 191-214.

Mogensen, T.E., 1995. Triassic and Jurassic structural development along the Tornquist Zone, Denmark. Tectonophysics 252, 197-220.

Morley, C.K., 1995. Developments in the structural geology of rifts over the last decade and their impact on hydrocarbon exploration. Geological Society, London, Special Publications 80, 1.

Neumann, E.-R., Wilson, M., Heeremans, M., Spencer, E.A., Obst, K., Timmerman, M.J., Kirstein, L., 2004. Carboniferous-Permian rifting and magmatism in southern Scandinavia, the North Sea and northern Germany: a review. Geological Society, London, Special Publications 223, 11-40.

Panien, M., Buiter, S., Schreurs, G., Pfiffner, O.-A., 2006. Inversion of a symmetric basin: insights from a comparison between analogue and numerical experiments. Geological Society, London, Special Publications 253, 253-270.

Panien, M., Schreurs, G., Pfiffner, A., 2005. Sandbox experiments on basin inversion: testing the influence of basin orientation and basin fill. Journal of Structural Geology 27, 433-445.

Patruno, S., Reid, W., Berndt, C., Feuilleaubois, L., 2019. Polyphase tectonic inversion and its role in controlling hydrocarbon prospectivity in the Greater East Shetland Platform and Mid North Sea High, UK. Geological Society, London, Special Publications 471, 177.

Pegrum, R.M., 1984. The extension of the Tornquist Zone in the Norwegian North Sea. Norsk Geologisk Tidsskrift 64, 39-68.

Pharaoh, T.C., 1999. Palaeozoic terranes and their lithospheric boundaries within the Trans-European Suture Zone (TESZ): a review. Tectonophysics 314, 17-41.

Phillips, T.B., Jackson, C.A., Bell, R.E., Duffy, O.B., Fossen, H., 2016. Reactivation of intrabasement structures during rifting: A case study from offshore southern Norway. Journal of Structural Geology 91, 54-73.

Phillips, T.B., Jackson, C.A.L., Bell, R.E., Duffy, O.B., 2018. Oblique reactivation of lithosphere-scale lineaments controls rift physiography – the upper-crustal expression of the Sorgenfrei–Tornquist Zone, offshore southern Norway. Solid Earth 9, 403-429.

Phillips, T.B., Jackson, C.A.L., Bell, R.E., Valencia, A.A., 2019. Rivers, reefs and deltas: geomorphological evolution of the Jurassic of the Farsund Basin, offshore southern Norway. Petroleum Geoscience, petgeo2018-2056.

Phillips, T.B., Magee, C., Jackson, C.A.L., Bell, R.E., 2017. Determining the three-dimensional geometry of a dike swarm and its impact on later rift geometry using seismic reflection data. Geology 46, 119-122.

Reilly, C., Nicol, A., Walsh, J., 2017. Importance of pre-existing fault size for the evolution of an inverted fault system. Geometry and Growth of Normal Faults 439, 447-463.

Rodríguez-Salgado, P., Childs, C., Shannon, P.M., Walsh, J.J., 2019. Structural evolution and the partitioning of deformation during basin growth and inversion: A case study from the Mizen Basin Celtic Sea, offshore Ireland. Basin Res n/a.

Salomon, E., Koehn, D., Passchier, C., 2015. Brittle reactivation of ductile shear zones in NW Namibia in relation to South Atlantic rifting. Tectonics 34, 70-85.

Sandiford, M., Hand, M., 1998. Controls on the locus of intraplate deformation in central Australia. Earth and Planetary Science Letters 162, 97-110.

Scisciani, V., Patruno, S., Tavarnelli, E., Calamita, F., Pace, P., Iacopini, D., 2019. Multi-phase reactivations and inversions of Paleozoic-Mesozoic extensional basins during the Wilson Cycle: case studies from the North Sea (UK) and Northern Apennines (Italy). Geological Society, London, Special Publications 470, SP470-2017-2232.

Sclater, J.G., Christie, P.A., 1980. Continental stretching: An explanation of the post-mid-Cretaceous subsidence of the central North Sea basin. Journal of Geophysical Research: Solid Earth 85, 3711-3739.

Skjerven, J., Rijs, F., and Kalheim, J.: Late Palaeozoic to Early Cenozoic structural development of the south-southeastern Norwegian North Sea, Petroleum Geology of the Southeastern North Sea and the Adjacent Onshore Areas, Springer, 35–45, 1983.

Sørensen, S., Morizot, H., Skottheim, S., 1992. A tectonostratigraphic analysis of the southeast Norwegian North Sea Basin, in: Larsen, R.M., Brekke, H., Larsen, B.T., Talleraas, E. (Eds.), Structural and Tectonic Modelling and its Application to Petroleum Geology. Elsevier, Amsterdam, pp. 19-42.

Sørensen, S., Tangen, O.H., 1995. Exploration trends in marginal basins from Skagerrak to Stord, in: Hanslien, S. (Ed.), Norwegian Petroleum Society Special Publications. Elsevier, pp. 97-114.

Stephenson, R., Egholm, D.L., Nielsen, S.B., Stovba, S.M., 2009. Role of thermal refraction in localizing intraplate deformation in southeastern Ukraine. Nature Geoscience 2, 290-293.

Suppe, J., 1983. Geometry and kinematics of fault-bend folding. American Journal of science 283, 684-721.

Tassone, D., Holford, S., Stoker, M.S., Green, P., Johnson, H., Underhill, J.R., Hillis, R., 2014. Constraining Cenozoic exhumation in the Faroe-Shetland region using sonic transit time data. Basin Res 26, 38-72.

Thybo, H., 2000. Crustal structure and tectonic evolution of the Tornquist Fan region as revealed by geophysical methods. Bulletin of the Geological Society of Denmark 46, 145-160.

Turner, J.P., Williams, G.A., 2004. Sedimentary basin inversion and intra-plate shortening. Earth-Science Reviews 65, 277-304.

Walsh, J.J., Childs, C., Meyer, V., Manzocchi, T., Imber, J., Nicol, A., Tuckwell, G., Bailey, W.R., Bonson, C.G., Watterson, J., Nell, P.A., Strand, J., 2001. Geometric controls on the evolution of normal fault systems. Geological Society, London, Special Publications 186, 157.

Williams, G.A., Turner, J.P., Holford, S.P., 2005. Inversion and exhumation of the St. George's Channel basin, offshore Wales, UK. Journal of the Geological Society 162, 97-110.

Wilson, M., Neumann, E.-R., Davies, G.R., Timmerman, M., Heeremans, M., Larsen, B.T., 2004. Permo-Carboniferous magmatism and rifting in Europe: introduction. Geological Society, London, Special Publications 223, 1-10.

Withjack, M.O., Schlische, R.W., 2006. Geometric and experimental models of extensional fault-bend folds. Geological Society, London, Special Publications 253, 285.

Wyllie, M.R.J., Gregory, A.R., Gardner, L.W., 1956. Elastic wave velocities in heterogeneous and porous media. Geophysics 21, 41-70.

Yamada, Y., McClay, K., 2004. 3-D analog modeling of inversion thrust structures.

Youash, Y., 1969. Tension Tests on Layered Rocks. Geological Society of America Bulletin 80, 303-306.

Ziegler, P.A., 1992. North-Sea Rift System. Tectonophysics 208, 55-75.

Figure 1: Conceptual model of the reverse reactivation of a previously extensional normal fault. Ductile folding occurs in the hangingwall of the fault producing an anticline displaying a constant amplitude with depth. Strata onlapping onto the limb of the fold at the free surface indicate the age of folding and therefore inversion. In the case of the Farsund Basin, the upper part of the anticline is eroded by the Base Pleistocene Unconformity, meaning that we have no constraints on the timing of inversion. Projected hangingwall cutoffs and the footwall cutoff used for throw analyses are also shown.

Figure 2: A) Regional two-way-time (TWT) structure map showing the top Acoustic Basement surface (typically base Triassic/base Zechstein Supergroup evaporites) across the region. The locations and calculated total uplift values of wells, used to constrain the ages of stratigraphic horizons across the area are shown. Grey lines indicate the locations of 2D seismic lines referred to in this study. Seismic data used to create the rest of the Acoustic Basement surface can be found in Phillips et al., (2016). Inset - Regional map showing the location of the study area and Sorgenfrei-Tornquist Zone. B) Tectonostratigraphic column for the Farsund Basin based on lithological information from well 11/5-1 (after Phillips et al., 2019), showing the main lithologies and tectonic events.

Figure 3: A) Interpreted N-S oriented seismic section highlighting the present geometry of the Farsund Basin. B) The same section flattened on the Base Jurassic Unconformity highlighting the rough structural and stratal geometries present at the beginning of the Jurassic. The Farsund Basin has not formed at this time and is contiguous with the Varnes Graben and Norwegian-Danish to the north and south, respectively. Triassic strata show only regional thinning towards the north, with salt mobilisation occurring down the paleoslope into the Norwegian-Danish Basin. See Figure 2 for location.

Figure 4: Schematic diagram showing how uplift is calculated by projecting truncated stratigraphy above an unconformity. Uplift estimates based on straight and modified projections of strata are calculated. Where possible, measurements are taken at the largest possible value, however, projections are not calculated across faults.

Figure 5: A) Two-way-time Structure map~~al~~ of the Acoustic Basement horizon ~~map~~ and seismic sections highlighting the characteristic structural style associated with each fault domain (A-D). Black lines show the location of individual domain sections. B) Throw-length profiles calculated across the Farsund North Fault for the Acoustic Basement, Base Jurassic Unconformity and Top Jurassic horizons. Background colours correspond to different domains. C) Calculated uplift values (red and black) calculated along the northern margin of the Farsund Basin through the projections of truncated strata. Blue lines show the amplitudes of the hangingwall inversion folds at various structural levels.

Figure 6: A) Lower Cretaceous porosity-depth data from seven wells in the region, including one from the Farsund Basin (11/5-1). Depth measured in metres below seabed (m bSB). A normal compaction curve for Norwegian Shelf Lower Cretaceous shales is also shown (Hansen, 1996a). B) Estimates of net exhumation (E_N) and gross exhumation (E_G), which takes into account the vertical thickness of supra-Pleistocene unconformity sediments (B_E). Also shown are values of E_G from earlier studies using different stratigraphic intervals from several of the same boreholes. The difference between these estimates of E_G and those calculated in this study are shown (E_g difference). See Figure 2 for the locations of each of the wells.

Figure 7: Interpreted seismic section across the Farsund Basin and Agder Slope, showing subcrop projections, taking into account underlying stratal geometries, and associated uplift. See Figure 2 for location.

Figure 8: Subcrop map across the Farsund Basin at the Base Pleistocene Unconformity. Black lines show the locations of faults that are truncated by the Base Pleistocene Unconformity, thick grey lines show fault geometries at the Acoustic Basement level. Thin grey lines show the location of 2D seismic sections used to create the map, with those referred to elsewhere in the study in red.

Figure 9: Uninterpreted and interpreted seismic sections highlighting the along-strike variability in fold geometry within Domain C. See Figure 5a for locations. A) Fold geometry in the west of Domain C showing a hangingwall anticline which decreases in amplitude upwards. B) Section from the centre of Domain C, note how lowermost Lower Cretaceous strata onlap onto the limb of the fold at deeper levels. C) Section from the east of Domain C, note how Lower Cretaceous strata thin onto the limb of the fold at deeper levels.

Figure 10: Interpreted seismic section across the centre of the Farsund Basin. See Figure 2 for location. Lower and Upper Cretaceous strata are truncated at the Base Pleistocene Unconformity and a series of low-displacement faults are developed in the centre of the basin.

Figure 11: Schematic model illustrating the inversion of a pre-existing fault propagation fold. A) An initial stage of fault propagation folding occurred during Early Cretaceous slip along the fault. Lower Cretaceous strata onlap onto the basinward-facing limb of the fold. B) Following further slip along the fault, the fault propagation fold becomes breached. C) Reverse reactivation of the fault and folding of hangingwall strata occurs during the Late Cretaceous. At shallow depths, this creates an inversion-related monocline, whereas at greater depths, the pre-existing monocline is tightened, forming a composite Early Cretaceous fault propagation and Late Cretaceous inversion-related fold.

Figure 12: The different styles by which compressional stresses are expressed along the Sorgenfrei-Tornquist Zone throughout Late Cretaceous and Neogene events. A) The STZ localises compression originating from the south, at upper crustal depths, this is buttressed against the Farsund North Fault via reverse reactivation and long-wavelength folding of hangingwall strata. Right - the STZ acts as a hinge line during the Neogene, separating areas of relatively low uplift in the Norwegian-Danish Basin, from the areas of relatively high uplift further north towards the Norwegian mainland.

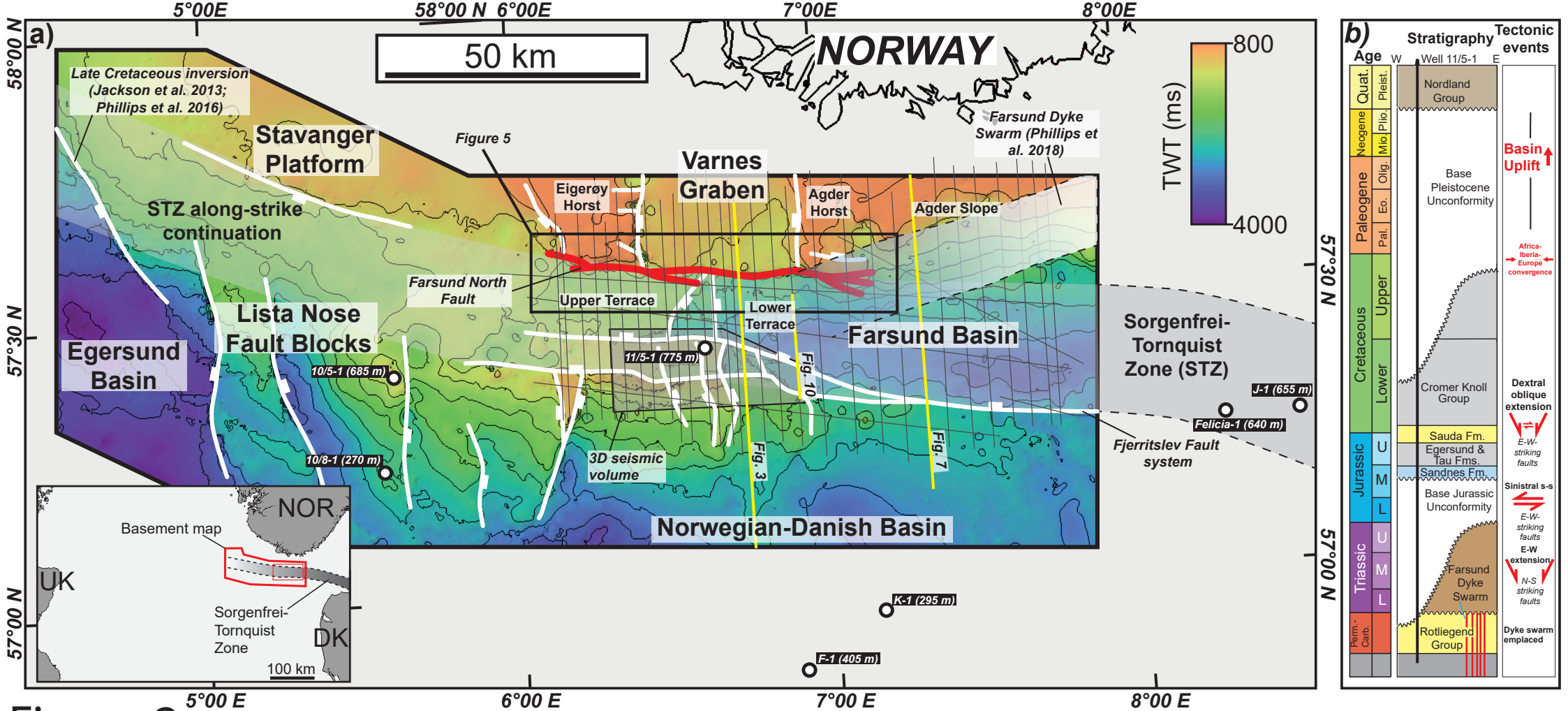
a)
50 km
NORWAY
TWT (ms)
800
4000
5°00E
58°00 N
6°00E
7°00E
8°00E
58°00 N
57°30 N
57°00 N
Late Cretaceous inversion (Jackson et al. 2013; Phillips et al. 2016)
Stavanger Platform
Figure 5
Varnes Graben
Eigerøy Horst
Agder Horst
Agder Slope
Farsund Dyke Swarm (Phillips et al. 2018)
STZ along-strike continuation
Farsund North Fault
Upper Terrace
Lower Terrace
Lista Nose Fault Blocks
Egersund Basin
Farsund Basin
Sorgenfrei-Tornquist Zone (STZ)
10/5-1 (685 m)
11/5-1 (775 m)
J-1 (655 m)
Felicia-1 (640 m)
10/8-1 (270 m)
Fig. 10
Fig. 7
Fig. 3
3D seismic volume
Fjerritslev Fault system
Norwegian-Danish Basin
K-1 (295 m)
F-1 (405 m)
Basement map
NOR
UK
DK
Sorgenfrei-Tornquist Zone
100 km
5°00 E
6°00 E
7°00 E
8°00 E
b)
Stratigraphy
Tectonic events
Age
W
Well 11/5-1
E
Quat.
Pleist.
Neogene
Plio.
Mio.
Paleogene
Olig.
Eo.
Pal.
Cretaceous
Upper
Lower
Jurassic
U
M
L
Triassic
U
M
L
Perm.-Carb.
Nordland Group
Base Pleistocene Unconformity
Cromer Knoll Group
Sauda Fm.
Egersund & Tau Fms.
Sandnes Fm.
Base Jurassic Unconformity
Farsund Dyke Swarm
Rotliegend Group
Basin Uplift
Africa-Iberia-Europe convergence
Dextral oblique extension
E-W-striking faults
Sinistral s-s
E-W-striking faults
E-W extension
N-S striking faults
Dyke swarm emplaced

Figure 2

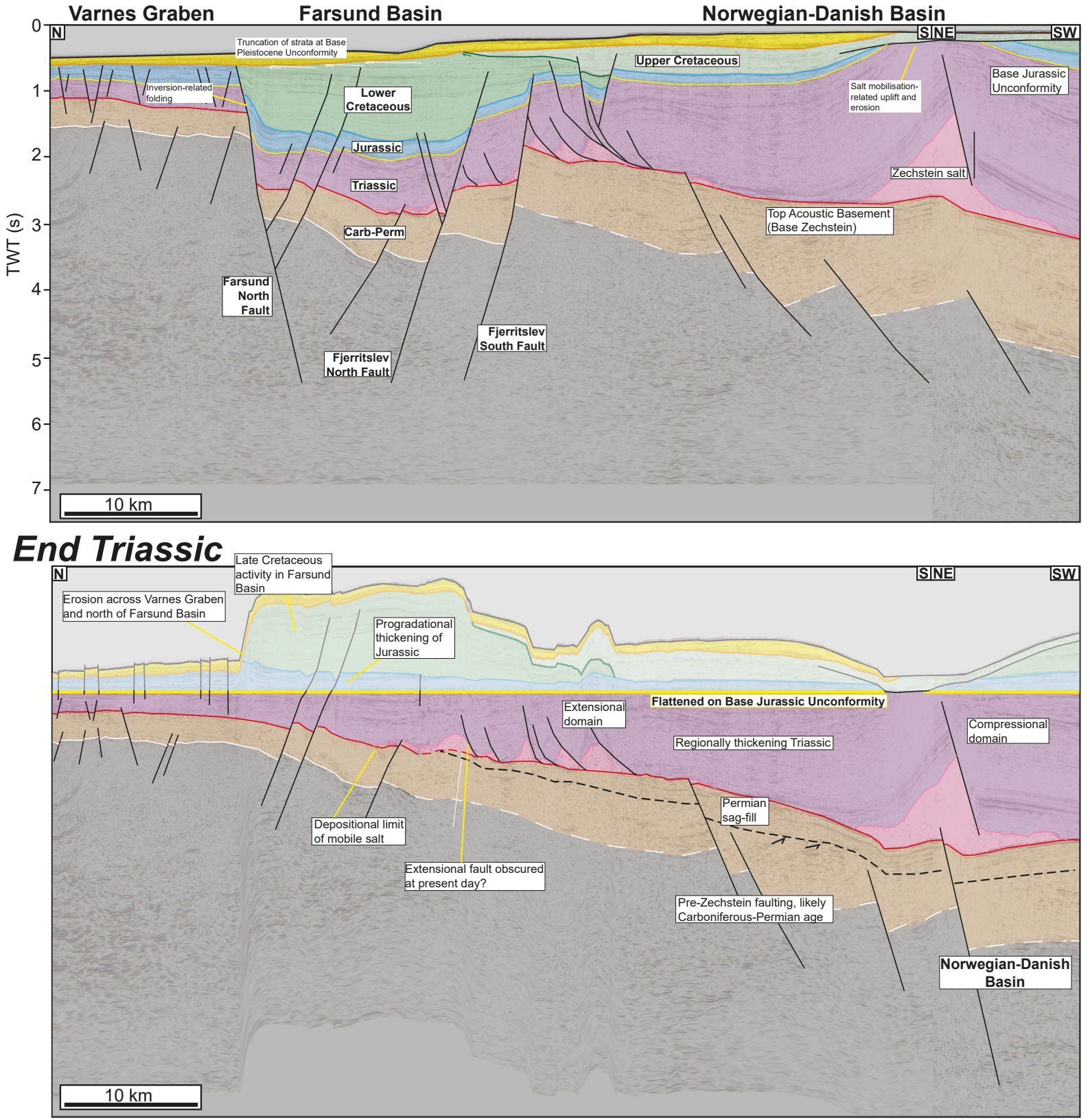
Varnes Graben
Farsund Basin
Norwegian-Danish Basin
N
S
NE
SW
TWT (s)
0
1
2
3
4
5
6
7
Truncation of strata at Base Pleistocene Unconformity
Upper Cretaceous
Base Jurassic Unconformity
Inversion-related folding
Lower Cretaceous
Salt mobilisation-related uplift and erosion
Jurassic
Zechstein salt
Triassic
Top Acoustic Basement (Base Zechstein)
Carb-Perm
Farsund North Fault
Fjerritslev South Fault
Fjerritslev North Fault
10 km
End Triassic
N
S
NE
SW
Late Cretaceous activity in Farsund Basin
Erosion across Varnes Graben and north of Farsund Basin
Progradational thickening of Jurassic
Flattened on Base Jurassic Unconformity
Extensional domain
Compressional domain
Regionally thickening Triassic
Permian sag-fill
Depositional limit of mobile salt
Extensional fault obscured at present day?
Pre-Zechstein faulting, likely Carboniferous-Permian age
Norwegian-Danish Basin
10 km

Figure 3

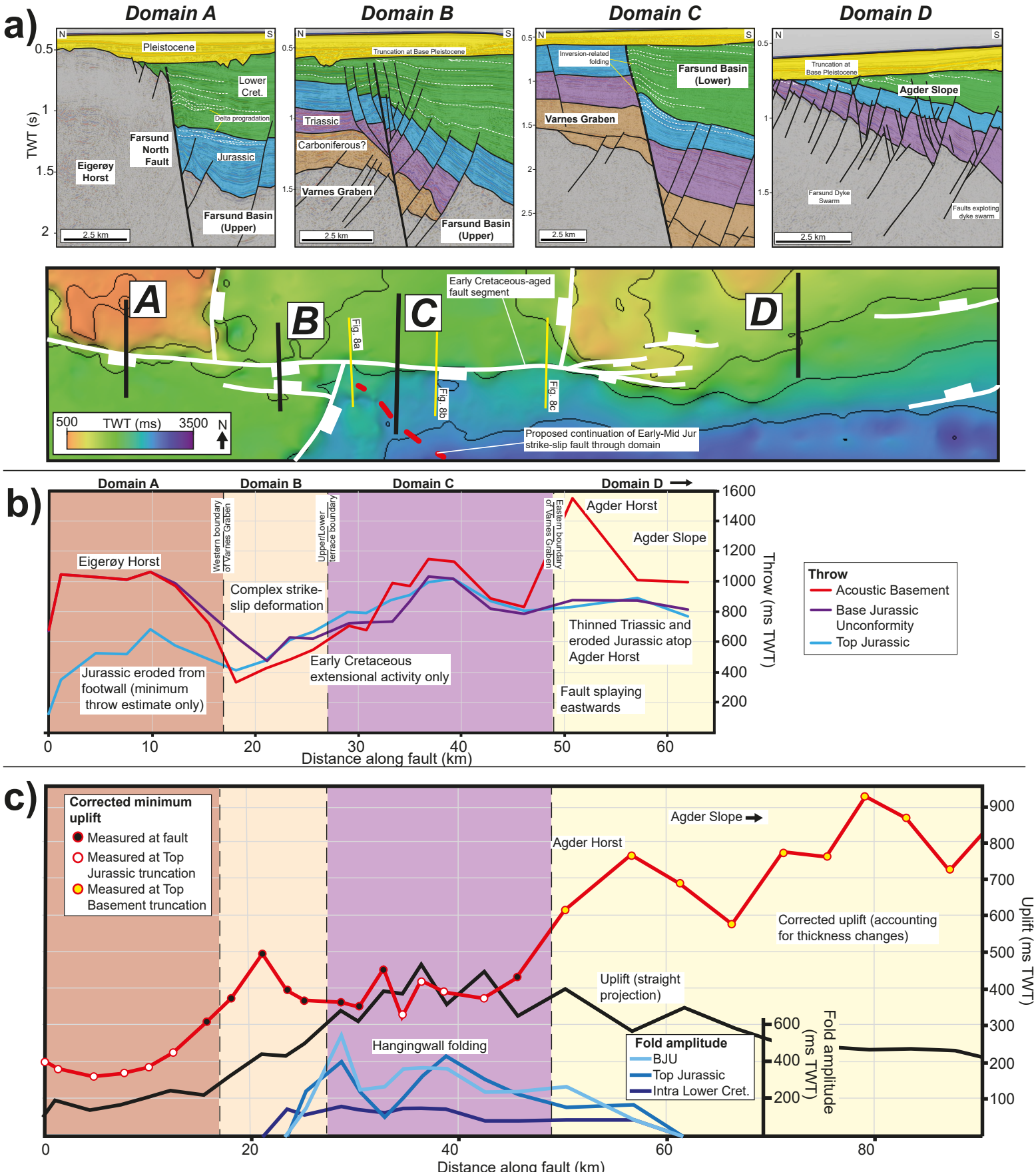
a)
Domain A
Domain B
Domain C
Domain D
N
S
TWT (s)
Pleistocene
Lower Cret.
Delta progradation
Farsund North Fault
Jurassic
Eigerøy Horst
Farsund Basin (Upper)
2.5 km
Truncation at Base Pleistocene
Triassic
Carboniferous?
Varnes Graben
Inversion-related folding
Farsund Basin (Lower)
Agder Slope
Farsund Dyke Swarm
Faults exploting dyke swarm
A
B
C
D
Fig. 8a
Fig. 8b
Fig. 8c
Early Cretaceous-aged fault segment
500
TWT (ms)
3500
Proposed continuation of Early-Mid Jur strike-slip fault through domain
b)
Western boundary of Varnes Graben
Upper/Lower Terrace boundary
Eastern boundary of Varnes Graben
Eigerøy Horst
Agder Horst
Agder Slope
Complex strike-slip deformation
Thinned Triassic and eroded Jurassic atop Agder Horst
Early Cretaceous extensional activity only
Jurassic eroded from footwall (minimum throw estimate only)
Fault splaying eastwards
Throw (ms TWT)
Distance along fault (km)
Throw
Acoustic Basement
Base Jurassic Unconformity
Top Jurassic
c)
Corrected minimum uplift
Measured at fault
Measured at Top Jurassic truncation
Measured at Top Basement truncation
Agder Slope
Agder Horst
Corrected uplift (accounting for thickness changes)
Uplift (straight projection)
Hangingwall folding
Fold amplitude
BJU
Top Jurassic
Intra Lower Cret.
Fold amplitude (ms TWT)
Uplift (ms TWT)
Distance along fault (km)

Figure 5

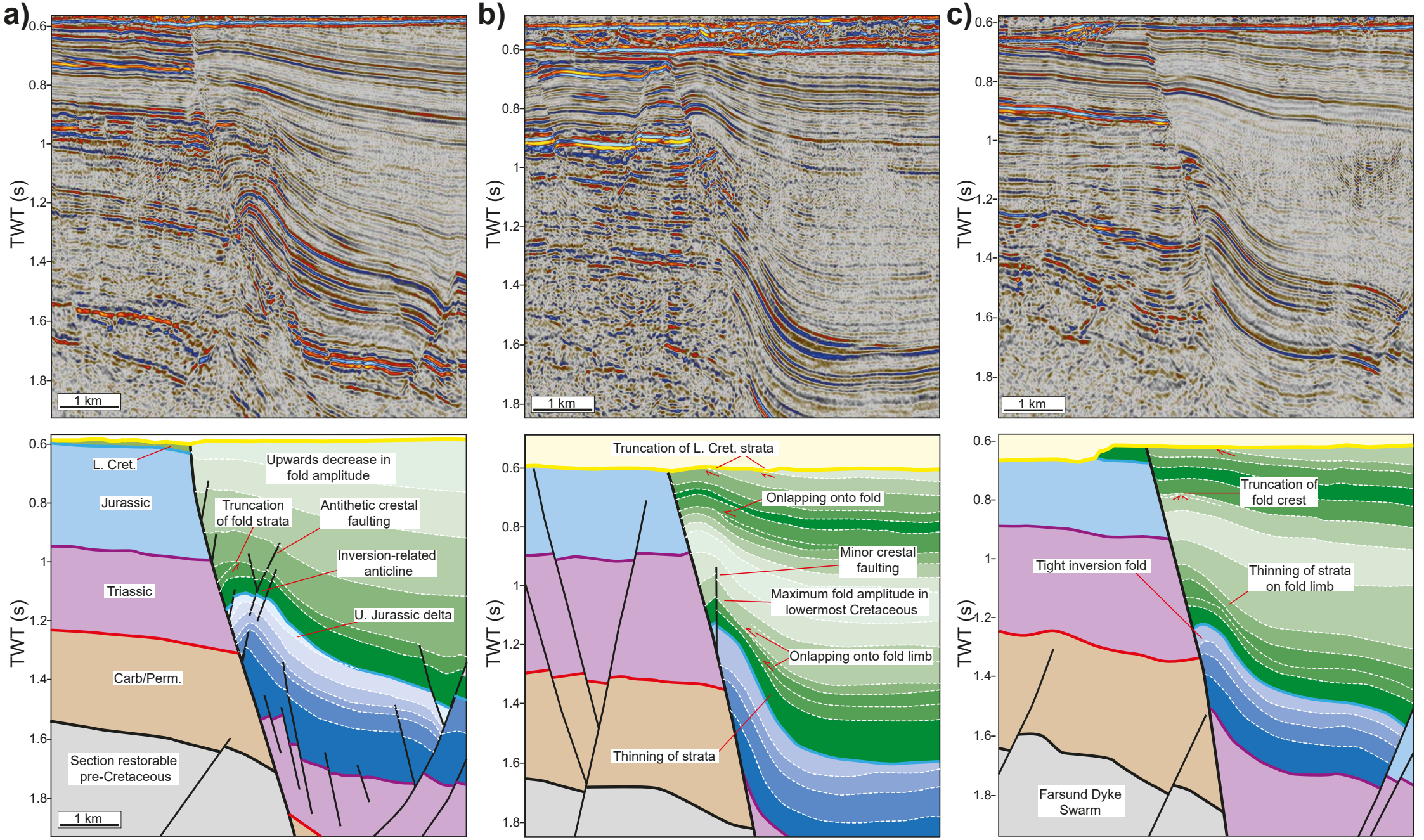
a)
b)
c)
TWT (s)
0.6
0.8
1
1.2
1.4
1.6
1.8
1 km
L. Cret.
Jurassic
Triassic
Carb/Perm.
Section restorable pre-Cretaceous
Upwards decrease in fold amplitude
Truncation of fold strata
Antithetic crestal faulting
Inversion-related anticline
U. Jurassic delta
Truncation of L. Cret. strata
Onlapping onto fold
Minor crestal faulting
Maximum fold amplitude in lowermost Cretaceous
Onlapping onto fold limb
Thinning of strata
Truncation of fold crest
Tight inversion fold
Thinning of strata on fold limb
Farsund Dyke Swarm

Figure 9

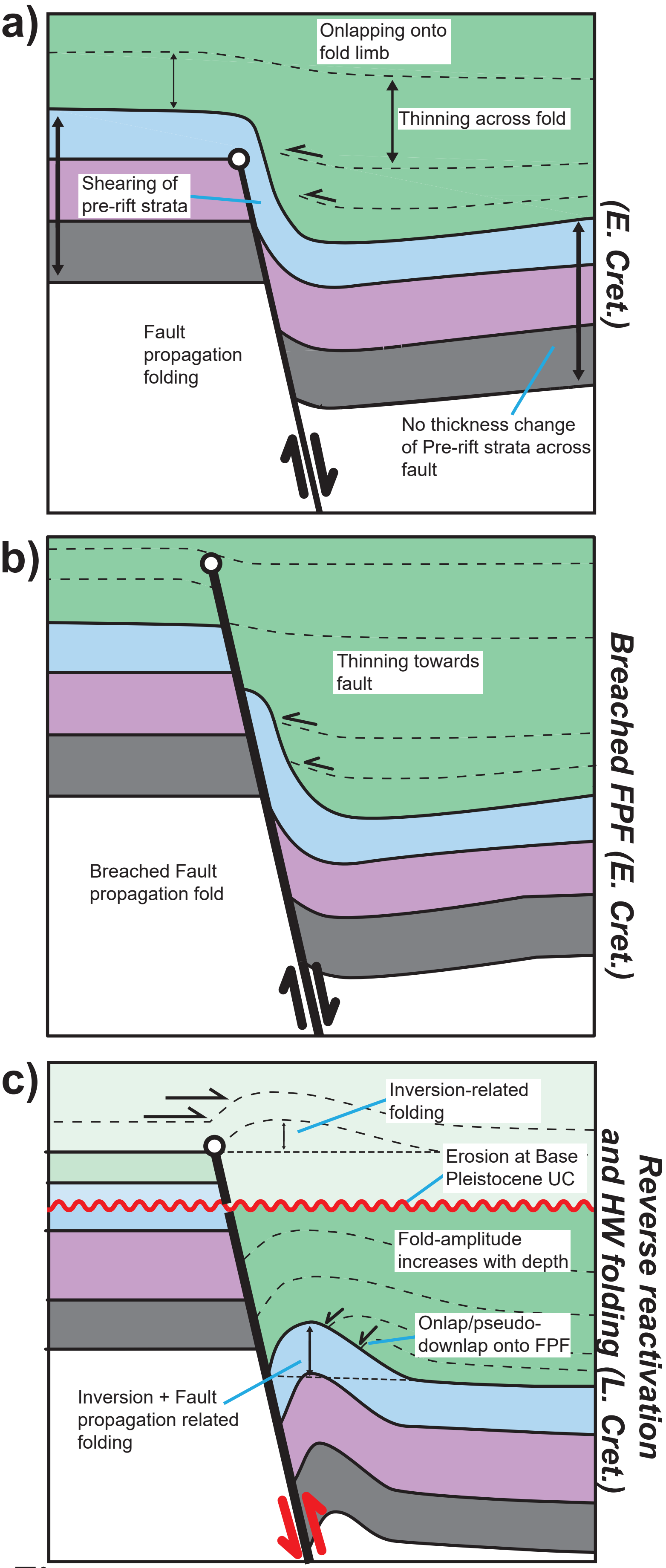
a)
Onlapping onto fold limb
Thinning across fold
Shearing of pre-rift strata
Fault propagation folding
No thickness change of Pre-rift strata across fault
(E. Cret.)
b)
Thinning towards fault
Breached Fault propagation fold
Breached FPF (E. Cret.)
c)
Inversion-related folding
Erosion at Base Pleistocene UC
Fold-amplitude increases with depth
Onlap/pseudo-downlap onto FPF
Inversion + Fault propagation related folding
Reverse reactivation and HW folding (L. Cret.)

Figure 11